

MEL: Multi-level Ensemble Learning for Resource-Constrained Environments

Krishna Praneet Gudipaty¹ Walid A. Hanafy¹ Kaan Ozkara² Qianlin Liang^{4*}

Jesse Milzman³ Prashant Shenoy¹ Suhas Diggavi²

¹University of Massachusetts Amherst, USA

²University of California, Los Angeles, USA

³Army Research Laboratory, USA

⁴Amazon, USA

ABSTRACT

AI inference at the edge is becoming increasingly common for low-latency services. However, edge environments are power- and resource-constrained, and susceptible to failures. Conventional failure resilience approaches, such as cloud failover or compressed backups, often compromise latency or accuracy, limiting their effectiveness for critical edge inference services. In this paper, we propose Multi-Level Ensemble Learning (MEL), a new framework for resilient edge inference that simultaneously trains multiple lightweight backup models capable of operating collaboratively, refining each other when multiple servers are available, and independently under failures while maintaining good accuracy. Specifically, we formulate our approach as a multi-objective optimization problem with a loss formulation that inherently encourages diversity among individual models to promote mutually refining representations, while ensuring each model maintains good standalone performance. Empirical evaluations across vision, language, and audio datasets show that MEL provides performance comparable to original architectures while also providing fault tolerance and deployment flexibility across edge platforms. Our results show that our ensemble model, sized at 40% of the original model, achieves similar performance, while preserving 95.6% of ensemble accuracy in the case of failures when trained using MEL.

1 Introduction

Edge AI has recently emerged as a complementary approach to cloud-based AI for running low-latency inference services, particularly due to the reduced network latency to access edge services from client devices [44, 26, 27, 43]. However, edge servers are often deployed as small modular data centers in harsh environments, such as the base of cell towers, making them more susceptible to hardware, connectivity, or power failures. Consequently, failures of edge AI services running on these platforms are likely to be more commonplace or more frequent than corresponding cloud-based services, necessitating the use of failure resilience techniques to withstand faults [48, 23]. However, conventional failure resilience techniques that are commonly used in cloud platforms do not work well in edge settings. For example, the conventional approach of using backup replica servers to take over inference tasks from primary servers that experience failures may be infeasible in edge data centers, since additional servers may be unavailable in such resource-constrained environments. Another approach is to use cloud resources, where the failure of one or more edge servers involves switching over to cloud servers [17], but doing so negates the latency advantage of edge inference. Yet another approach involves running a compressed version of the primary model on the limited resources available on a backup edge server and switching to the compressed model upon failure [55]. However, the size of a *single* compressed backup model may be severely limited in resource-constrained environments, and

*Work done while Qianlin Liang was a Ph.D. student at the University of Massachusetts Amherst.

doing so can degrade inference accuracy upon a failure. Thus, conventional approaches for handling edge failures come with several limitations.

To address the issue of failover in resource-constrained environments, we propose a novel *multi-level ensemble learning* methodology that can gracefully degrade performance with increasing failures. Our solution is motivated by the fact that while resources may be too constrained to run a single performant backup model, combining resources from different servers (*e.g.*, by piggybacking on multiple servers) can allow us to achieve reasonable performance. In particular, the goal of multi-level ensemble learning (MEL) is to design models that: 1) refine each other so as to get better performance when combined (*i.e.*, when more resources are available) and 2) are individually good to make the system more robust in case of failures. In this paper, we investigate the approach of using multiple (*i.e.*, two or more) such small failover backup models, which refine each other when combined. For example, we can use two small backup models $h_{\{1\}}, h_{\{2\}}$, which are placed on two different edge servers 1 and 2, and are invoked when the main model h_{main} fails. Now, if the main server fails and only one of the two edge servers work, then we want an inference with just one of the small models; therefore for the backup models want “reasonable” performance individually. One trivial solution is to duplicate the small backup model in edge servers 1 and 2, and design it to get “reasonable” performance; however, in the event that both of the backup servers are available, then we do not gain any advantage. Therefore, the paper is focused on addressing the question of ensuring that the ensemble models are *diverse* so that they provide better performance when combined, while also providing reasonable performance individually.

Note that this is different from the popular mixture-of-experts paradigm [47], where the individual learners are experts in certain aspects, and can perform very poorly in others. In contrast, we need the individual models to be reasonable learners in all aspects. Therefore, the first challenge to address is the loss criterion to be optimized to ensure such a design, for example, how to encourage diversity in the individual models; we will explore this in Section 2. The second challenge is to design the architecture and characteristics of the ensemble to be used for training to achieve the above properties; we will explore this in Section 3.

Contributions. Our contributions can be summarized as follows:

- We formalize MEL, a framework that jointly trains multiple lightweight backup models via a weighted combined training objective that also supports hierarchical labeling. MEL is deployed with a fail-aware inference protocol that enables graceful performance degradation. Furthermore, we provide an information-theoretic generalization bound linking model diversity to complexity.
- We design the architecture of our ensemble models by using prefix blocks of the primary model architecture and detail the design space for selecting a suitable ensemble structure, as well as the runtime considerations.
- We extensively evaluate MEL across vision and audio datasets, showing our design flexibility across different resource constraints. Our results show that our ensemble model, sized at 40% of the original model, achieves similar performance, while preserving 95.6% of ensemble accuracy in the case of failures.
- Lastly, we implemented a failure-resilient inference service based on our proposed architecture. Our evaluation in real edge settings showed that our MEL approach not only achieves higher resilience than baseline approaches but also achieves 25% less inference time.

Related work. In MEL, we propose a different approach that trains an ensemble of models capable of running cooperatively and independently, providing higher resilience guarantees. The prior work related to these aspects is addressed in this section.

AI Inference Systems. AI inference systems allow users to deploy their models in the cloud, edge, and on-device platforms. Tools such as Nvidia Triton [36], Kubeflow [25], TensorFlow Serving [37], TVM [8], and ONNX Runtime [35] allow users to deploy DNN models on a cluster of multiple cloud or edge resources. Building on these tools, researchers have focused on optimizing the inference latency and cost [9, 13, 48, 62, 41, 61, 27, 13, 59, 2, 16, 29] and addressing challenges of workload dynamics [1, 2, 60, 52, 28]. MEL builds on these efforts and addresses the issue of failure resiliency that has not seen much attention, especially in resource-constrained environments.

Failure Resiliency in Resource-constrained Environments. In cloud platforms, resources are abundant, and traditional failure resiliency approaches, such as replication, can be employed. For instance, in [48], the author replicates every request to optimize the latency and ensure failure resiliency. In contrast, edge environments, which are more prone to power and hardware failures than cloud resources, as they are typically deployed in remote and sometimes hostile environments, are highly resource-constrained, rendering such replication approaches inapplicable. A widely accepted strategy for ensuring failure resilience in resource-

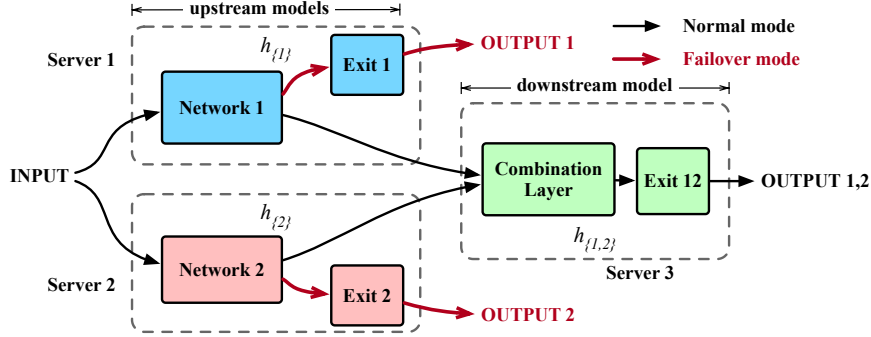


Figure 1: An example *multi-level ensemble* architecture featuring two upstream models and a downstream model comprising a combination and exit layers. The figure also highlights the data flow in the normal mode, where servers 1,2, and 3 are available, and in the failover mode, where either one of the servers or the combination server (i.e., server 3) fails.

constrained environments is graceful degradation [64, 34, 23, 17], which often involves sacrificing performance by limiting the available functionalities. For example, [34, 64] allocates resources according to the criticality of applications, reducing the number of services and functions available during failures. In the context of AI inference, researchers have focused on two main techniques. The first approach involves model compression and selection [55, 17], where models are substituted with smaller backups that usually use fewer resources but offer lower accuracy. In this case, when the primary (*i.e.*, large) model fails, the inference requests are redirected to a small failover replica. The second approach utilizes early-exit and skip-connection to horizontally split models processing across servers to guarantee a result is produced even when one or more servers fail [57, 58, 32]. In contrast to these approaches, MEL trains an ensemble model capable of harnessing resources across multiple servers. MEL provides a complementary approach, where users can select the ensemble size and allow for the sub-models to be placed on different servers.

Ensemble Learning. Early ensemble methods such as Bagging [5], AdaBoost [12] and Random Forests [6] established that aggregating diverse base learners reduces variance and boosts accuracy by voting or averaging predictions. These approaches inspired a large body of work on model aggregation, stacking that remains a cornerstone of statistical learning theory. However, they do not consider resilience or robustness towards failures of individual learners. Orthogonally, Mixture-of-Experts (MoE) architectures route each input through a subset of specialist subnetworks, achieving conditional computation and massive parameter scaling. MoE dates back to [22], recently [47] transformed MoE from a modest modular learner into a scalable conditional-compute layer by introducing sparse top-k routing with load-balancing regularizers and an efficient parallel implementation, enabling trillion-parameter-level capacity at roughly the cost of a dense baseline. MoE, as the name suggests, is made up of ‘experts’ that specializes according to inputs. In contrast, in MEL, we require each learner to be generalizable to inputs so that the failure of a learner is not catastrophic (as it would be in MoE).

2 Problem Formulation

To formalize the MEL problem, let \mathbf{x} be inputs to the learning model and y be the labels associated with it in the supervised learning framework. We will consider learning models under a loss function $\ell(h(\mathbf{x}), y)$, where $h(\mathbf{x})$ is the prediction by model h for input \mathbf{x} . Conventionally, the performance is measured by the population risk as $L(h) = \mathbb{E}_{(\mathbf{x}, y) \sim \mathcal{P}}[\ell(h(\mathbf{x}), y)]$, for an unknown underlying distribution \mathcal{P} , and the model h is optimized over a hypothesis class $h \in \mathcal{H}$.

In our problem we are simultaneously training multiple models $\{h_{\mathcal{S}}\}$, where $\mathcal{S} \subseteq \mathcal{M} = \{1, \dots, M\}$, where we would like to ensure that the performance of each of the models is maintained while refining each other. That is, we would like to design $\{h_{\mathcal{S}}\}$ such that the population risks $L(h_{\mathcal{S}}) \leq \gamma_{\mathcal{S}}$, where we also want $\gamma_{\mathcal{S}} \leq \gamma_{\mathcal{S}'}$ if $\mathcal{S}' \subset \mathcal{S}$, *i.e.*, we have refinement in performance when we have access to more backup servers. To make this concrete, from Figure 1, we have two backup servers, and the individual models are $h_{\{1\}}, h_{\{2\}}$, and when both backup models succeed, they feed into another server which can build a model $h_{\{1,2\}}$, which takes intermediate representations from $h_{\{1\}}, h_{\{2\}}$ and does further processing to produce the final inference. The goal is to simultaneously train $h_{\{1\}}, h_{\{2\}}, h_{\{1,2\}}$ for the desired individual performances. We will use the

terminology upstream model for the models that feed into later downstream models; for *e.g.*, in this case $h_{\{1\}}, h_{\{2\}}$ are upstream models feeding into the downstream model $h_{\{1,2\}}$.

Objective: Note that we also want the model classes to be smaller (or less complex) for smaller subsets, *i.e.*, $h_{\mathcal{S}} \in \mathcal{H}_{\mathcal{S}}$ and the parametrization of $\mathcal{H}_{\mathcal{S}}$ is smaller if \mathcal{S} is smaller. Clearly, this leads to several natural questions (i) how do we compose the models $\{h_{\mathcal{S}}\}$, *i.e.*, what is exchanged between the upstream models and the downstream models? (ii) how do we choose the individual model classes $\mathcal{H}_{\mathcal{S}}$, *i.e.*, architect the system (iii) how do we train the models to satisfy these requirements? (iv) can we say anything about generalization performance bounds for this problem setup?

Training criterion: We will address (i) and (ii) in Section 3, but will set up the framework for (iii) and (iv) in this section next. Clearly to simultaneously find the models $\{h_{\mathcal{S}}\}$, it is a multi-objective optimization. For example we can setup

$$\min_{\{h_{\mathcal{S}} \in \mathcal{H}_{\mathcal{S}}\}} L(h_{\mathcal{M}}) \text{ such that } L(h_{\mathcal{S}}) \leq \gamma_{\mathcal{S}}, \mathcal{S} \subseteq \mathcal{M} = \{1, \dots, M\} \quad (1)$$

As is conventional, we solve this by replacing the population risks by their empirical risks, and therefore we formulate this as a Lagrangian as follows:

$$\mathcal{L} = \sum_{\mathcal{S} \subseteq \mathcal{M}} \lambda_{\mathcal{S}} \hat{L}(h_{\mathcal{S}}), \quad (2)$$

where $\{\lambda_{\mathcal{S}}\}$ define the Lagrangian weights and we have defined the empirical risks over a labeled dataset $\mathcal{D} = \{(\mathbf{x}_1, y_1), \dots, (\mathbf{x}_N, y_N)\}$ as

$$\hat{L}(h_{\mathcal{S}}) = \frac{1}{N} \sum_{i=1}^N \ell(h_{\mathcal{S}}(\mathbf{x}_i^{(\mathcal{S})}), y_i^{(\mathcal{S})}). \quad (3)$$

Note that we are allowing ourselves the flexibility to “process” the dataset \mathcal{D} to produce datasets $\mathcal{D}^{(\mathcal{S})} = \{(\mathbf{x}_1^{(\mathcal{S})}, y_1^{(\mathcal{S})}), \dots, (\mathbf{x}_N^{(\mathcal{S})}, y_N^{(\mathcal{S})})\}$. For example the processing we investigate in this paper is to “coarsify” the labels to produce $\{y_i^{(\mathcal{S})}\}$, *i.e.*, can take the CIFAR-100 dataset and use their 20 coarser superclass labels. One could also compress the inputs $\{\mathbf{x}_i\}$ to produce the hierarchy specific inputs $\{\mathbf{x}_i^{(\mathcal{S})}\}$. Therefore, our overall optimization problem to simultaneously find the models $\{h_{\mathcal{S}}\}$ from (2) becomes,

$$\min_{\{h_{\mathcal{S}} \in \mathcal{H}_{\mathcal{S}}\}} \sum_{\mathcal{S} \subseteq \mathcal{M}} \lambda_{\mathcal{S}} \hat{L}(h_{\mathcal{S}}). \quad (4)$$

The coefficients $\{\lambda_{\mathcal{S}}\}$ capture the relative importance of the multiple levels of this ensemble learning problem. Let us take a concrete example of $\mathcal{M} = \{1, 2\}$, and the problem then becomes $\min_{h_{\{1\}}, h_{\{2\}}, h_{\{1,2\}}} \{\lambda_1 \hat{L}(h_{\{1\}}) + \lambda_2 \hat{L}(h_{\{2\}}) + \lambda_{12} \hat{L}(h_{\{1,2\}})\}$. If we increase λ_{12} relative to λ_1, λ_2 then we want to encourage the individual models $h_{\{1\}}, h_{\{2\}}$ to be “different”/“diverse” so that they can be mutually refined to produce better performance for the downstream model $h_{\{1,2\}}$.

Inference time operation: During training, we need to simultaneously design $\{h_{\mathcal{S}}\}$ to be prepared for any configuration of failures at inference time. However, at inference time we have access to knowledge of the failures and we activate the appropriate backup models. For example, if the main server allocated to the task fails, so does its model h_{main} . Then we know which subset \mathcal{S} of backup servers have succeeded, and hence know which model $h_{\mathcal{S}}$ can be used. At inference time, we can operate with the full precision input \mathbf{x} and feed it to the model $h_{\mathcal{S}}$.

Learning theoretic setup. For simplicity we utilize the framework initiated in [56]¹. We consider an instance space \mathcal{Z} , a dataset $\mathcal{D} = \{\mathbf{Z}_i\}_{i=1}^n$ where $(\mathbf{x}_i, y_i) = \mathbf{Z}_i \in \mathcal{Z}$ and each sample is sampled from an underlying distribution \mathcal{P} , *i.e.*, $\mathbf{Z}_i \sim \mathcal{P}$, a hypothesis space \mathcal{H} , and a non-negative loss function $\ell : \mathcal{H} \times \mathcal{Z} \rightarrow \mathbb{R}^+$. A learning algorithm tries to output a hypothesis h such that population loss $L(h) := \mathbb{E}_{\mathbf{Z} \sim \mathcal{P}}[\ell(h, \mathbf{Z})]$ is minimized. As \mathcal{P} is unknown, empirically, we utilize the dataset \mathcal{D} to minimize empirical risk, $\hat{L}(h) := \frac{1}{n} \sum_{i=1}^n \ell(h, \mathbf{Z}_i)$. Then, the generalization error can be characterized as $\text{gen}(\mathcal{P}, P_{h|\mathcal{D}}) := E_{h, \mathcal{D}}[L(h) - \hat{L}(h)]$, where $P_{h|\mathcal{D}}$ is the conditional distribution of output hypothesis given the input dataset.

[56], obtains a generalization bound that relates mutual information between the hypothesis and dataset to generalization performance.

¹Following this work, there are important works [38, 18, 49, 7, 40, 14] using conditional mutual information (CMI), which we do not focus on for simplicity. However, we believe CMI results can be translated to our work.

Lemma 2.1 (Theorem 1 in [56]). *Given that $l(h, Z)$ is σ -sub-Gaussian for all $h \in \mathcal{H}, Z \sim \mathcal{P}$ we have,*

$$(\text{gen}(\mathcal{P}, P_{h|\mathcal{D}}))^2 \leq \frac{2\sigma^2}{n} I(\mathcal{D}; h).$$

In our setting we consider a Markov graph (see graph in Appendix) with 4 nodes in the form of $\mathcal{D} \rightarrow h_{\{1\}}, h_{\{2\}} \rightarrow h_{\{1,2\}}$, where individual hypotheses may be from different spaces $\mathcal{H}_1, \mathcal{H}_2, \mathcal{H}_{1,2}$; note given \mathcal{D} , $h_{\{1\}}$ and $h_{\{2\}}$ are independent. As a result can relate the generalization error with the mutual information $I(h_{\{1\}}; h_{\{2\}})$ as in the next theorem,

Proposition 2.1. *We consider overall generalization error $\text{gen}_{\text{overall}}^2 := \mathbb{E}_{\mathcal{D}, h_{\{1\}}, h_{\{2\}}, h_{\{1,2\}}} [L(h_{\{1,2\}}, h_{\{1\}}, h_{\{2\}})] = \mathbb{E}[\frac{1-p}{1+p}(L(h_{\{1,2\}}) - \hat{L}(h_{\{1,2\}}))^2 + \frac{p}{1+p}(L(h_{\{1\}}) - \hat{L}(h_{\{1\}}))^2 + \frac{p}{1+p}(L(h_{\{2\}}) - \hat{L}(h_{\{2\}}))^2]$, where $0 \leq p \leq 1$ acts as a failover probability, i.e. when $p = 1$ it is guaranteed to use a lightweight model, and $p = 0$ it is guaranteed to use the ensemble model. Then the overall generalization error (sum of squares) yields the following upper bound,*

$$\text{gen}_{\text{overall}}^2 \leq \frac{1}{1+p} \frac{2\sigma^2}{n} ((I(\mathcal{D}; h_{\{1\}}) + I(\mathcal{D}; h_{\{2\}})) - (1-p)(I(h_{\{1\}}; h_{\{2\}})))$$

Remark. The generalization error is tightly related to the model complexity/capability. A more capable model is also capable of resulting higher generalization error due to overfitting risk [46]. In this remark, we tie the diversity of $h_{\{1\}}, h_{\{2\}}$ to model complexity through the generalization error [21]. We observe that the generalization error depends on $I(h_{\{1\}}; h_{\{2\}})$, the overall complexity of the architecture can be characterized through the mutual information of $h_{\{1\}}$ and $h_{\{2\}}$. When $I(h_{\{1\}}; h_{\{2\}})$ is small, i.e. $h_{\{1\}}$ and $h_{\{2\}}$ likely to output more diverse hypotheses, we observe that generalization error upper bound is increased indicating the increase in complexity as expected. And when $I(h_{\{1\}}; h_{\{2\}})$ is high it means $h_{\{1\}}$ and $h_{\{2\}}$ highly related and convey ‘similar’ information in the downstream channel, this indicates the overall architecture is less capable (complex) and the generalization error is decreased. Note that, given a capable model, overfitting can be mitigated through increasing/diversifying dataset. Furthermore, even though our method increases the generalization upper bound, we have *population risk = empirical risk + generalization error*; hence, if empirical loss is decreased sufficiently due to increased capability, we can still observe decreased population risk.

3 System Architecture

In this section, we explain how we instantiate the ensemble model h_S (i.e., question (i)) and explain the design space and run-time considerations (i.e., question (ii)) from Section 2.

Ensemble Architecture. Our multi-level ensemble $\{h_S\}$ features multiple upstream and downstream models as depicted in Figure 1. We base the architecture of our upstream models on the concept of *neural block*, or *block* for short, a commonly used approach in designing modern neural networks [19, 50]. Similar to multi-exit [28, 45, 51] and split processing approaches [20, 4, 33, 42], we design the upstream models by considering the original model and selecting a prefix of its blocks. For example, since the EfficientNet-B0 architecture comprises seven blocks, each with one or more convolution layers, we can design the smaller upstream models as a subset of blocks using a prefix of the original model architecture, which limits our design space to a discrete set of options. Additionally, we attach an exit block (e.g., classification layer) to each upstream model that is trained as part of the ensemble and only activated in cases of failures. Further, in contrast to early-exit or split processing, where subsequent phases or blocks rely on a single source of intermediate representation, our architecture combines intermediate representations from multiple complementary sources. Hence, our downstream model primarily contains a combination layer and output layer, but may feature a more complex architecture as we highlight in Appendix E. Lastly, as described in Section 2, we train the ensemble by considering a multi-objective training criterion that considers the accuracy of upstream models, their diversity, and the accuracy of the downstream model.

Design Space and Considerations. Several design decisions govern the training of a multi-level ensemble model for a specific edge deployment scenario. We discuss the design space and the runtime considerations for these design decisions below, with additional details in Appendix B.

- Our *first* design decision is the size and number of the upstream models, as both factors are key to their learning ability and resiliency. Since our approach uses the granularity of a block, only a discrete (and

Table 1: Summary of Evaluated Datasets

Task	Dataset	Description	Coarse Labels
Image Classification	CIFAR 100 [24]	60K 32×32 images	True (20 super classes)
	Tiered-ImageNet [39]	774K (subset of ImageNet-1k [10])	True (34 super classes)
Audio Classification, Speech recognition	Speech Commands [53]	65K (1-sec) recordings at 16kHz	False
LLM Pre-Training	BookCorpus [63]	11K novels comprising of 1.2B tokens	False

finite) set of choices is available to determine the number and sizes of upstream models. For example, the first block of a given architecture yields the smallest size upstream model h_i . In particular, our approach considers the available resources per server and selects a prefix subset of blocks based on this resource availability. As we demonstrate in Figure 3, since the model size significantly impacts the accuracy and larger sizes come with diminishing returns, picking a model size based on the knee of the curve yields a good balance between size and accuracy. Additionally, increasing the number of upstream models increases training complexity but also enables the system to tolerate more failures.

- Our *second* design decision is the size of the downstream model. While system resource constraints play an important role in determining the model size, they are not the only factor influencing our design. Resource fragmentation can also play a critical role since the available resource budget may not be evenly split across servers. In such scenarios, a key aspect of our design is how to apportion the total available resource between the upstream and downstream models. On one hand, allocating more resources to the upstream model creates performant models that benefit less from being combined; on the other hand, allocating more resources to the downstream model creates models dependent on the availability of the combination model.
- Our *third* decision is the relative importance of the upstream and downstream models, determined by the coefficients λ_S . The relative importance determines the model’s behavior in different scenarios. For instance, a higher weight for the downstream models encourages the ensemble model to produce “different” or “diverse” models that refine each other and increase its accuracy. In contrast, a higher weight for the upstream models trains more independent models that may not provide benefits when combined. The relative importance is also essential for determining the system’s resiliency under different failure types and the expected availability of different servers. For instance, in scenarios where network connectivity is intermittent, larger (i.e., more independent) upstream models are more adequate as they are less affected by connectivity failures.
- Our *fourth* design decision is the output granularity, where users can opt for results that represent slightly different (i.e., less complex) problems. One particular aspect that we focus on is to “coarsify” the output labels, which allows the model to yield higher accuracy, even in severely constrained environments, as we show in Table 4. For example, users can choose only to consider a binary classifier rather than a multi-class classifier, or classify the image as an animal as opposed to whether it is a dog or a cat.

In Section 4, Appendix D, Appendix E, we investigate the impact of the above design decisions and show the accuracy and the associated resource requirements of different design points.

MEL Deployment. In evaluating the performance of MEL, we implement a failure-resilience inference service. Since, from a practical standpoint, resource availability and failures are not known a priori at training time, our approach trains a family of multi-level ensembles, each for a different structure and resource requirements. In this case, at runtime, users or servers employ failure detection mechanisms (e.g., via heartbeat and timeouts). If the primary model fails, the users can choose the most appropriate ensemble to deploy in a particular edge environment via a best-fit approach. We detail our system implementation in Appendix B and depict the performance of an exemplar deployment in Figure 4.

4 Evaluation

In this section, we extensively evaluate the performance of MEL by comparing it across baselines. We start with an experimental setup, then introduce the evaluation results, followed by an ablation study of different configurations and scenarios.

4.1 Experimental Setup

Datasets. We evaluate our approach on the datasets listed in Table 1, (1) CIFAR-100 [24], consisting of 60K images across 100 fine-grained classes grouped into 20 superclasses, (2) Tiered ImageNet [39], a 700K-image

Table 2: The ensemble model $h_{\{1,2\}}$ matches the original model’s accuracy score on CIFAR-100, while preserving robustness and individual performance of $h_{\{1\}}$ and $h_{\{2\}}$.

DNN Model	MEL						Original	
	$h_{\{1\}}$		$h_{\{2\}}$		$h_{\{1,2\}}$		Acc.	Para.
	Acc.	Para.	Acc.	Para.	Acc.	Para.		
EfficientNet-B0 ($\mathcal{B}5$)	0.7371	0.88M	0.7428	0.88M	0.7769	1.79M	0.7763	4.79M
Resnet50 ($\mathcal{B}3$)	0.7324	8.76M	0.7043	8.76M	0.7552	17.50M	0.7593	23.93M

subset of ImageNet-1k [10] with 608 classes organized into 34 high-level categories, (3) Speech Commands [53], which contains 65K one-second audio recordings for keyword classification and speech recognition tasks, and (4) BookCorpus / [63], which is comprised of 11K novels and converted to 1.2 billion tokens using a tokenizer with a vocab size of 8K.

DNN Architectures. We utilize a multitude of DNN architectures to evaluate the performance of our multi-level ensemble learning methodology. In particular, we use EfficientNet-B0 [50], Resnet50 [19], ViT-B/16 [11], and DeepSpeech2 [3]. Our experiments denote these architectures as *original*, and construct our multi-level ensemble models using sub-blocks of these models as explained in Section 3. To establish notation, we refer to ensemble models by their architecture and the number of blocks used, as our current evaluation only focuses on fully connected downstream models. For example, EfficientNet-B0 ($\mathcal{B}3$), denotes an ensemble architecture with upstream models that uses first three layers of EfficientNet-B0.

Baselines. Our evaluation considers the following baselines: (1) the **original** architecture (for e.g. full-size Efficient-B0), which defines the target downstream model performance (2) a **small** failover replica, with the same size as $h_{\{1\}}$, serving as a baseline for conventional lightweight failover models [17, 55] (3) the **standalone** version of the $h_{\mathcal{S}}$ architecture, where only $h_{\{1,2\}}$ is optimized—serving as a benchmark for downstream accuracy when no constraints are imposed on upstream models (i.e., $\lambda_1 = \lambda_2 = 0$), and (4) an **individually-trained** ensemble, where the upstream models $h_{\{1\}}, h_{\{2\}}$ are trained independently in the first stage, followed by downstream training of $h_{\{1,2\}}$ with frozen weights in the upstream models, representing an alternative way to define $h_{\mathcal{S}}$ by combining representations post hoc, in contrast to the joint optimization used in MEL.

Training Details. In addition to the joint optimization proposed by MEL, we also fine-tune the downstream model while freezing upstream models to further improve accuracy, which will be discussed in the following sub-section. All models are implemented using PyTorch v2.5.1 and optimized using AdamW [31] under a cosine learning rate scheduler [30]. Lastly, the assessment of the system performance and response time of DNN inference services based on these models is done using ONNX Runtime v1.21, gRPC v1.71 on a local cluster of three Nvidia A2 GPUs. Full details of our setup, models, and datasets are available in Appendix C.

4.2 Experimental Results

In this section, we present the experimental results of MEL, focusing on ensembles composed of *two* upstream models. Appendix D presents the full results of MEL across architectures and datasets.

Initial Evaluation. Table 2 illustrates the results of our training approach using CIFAR-100 with EfficientNet-B0 ($\mathcal{B}5$), i.e., using the first five blocks, and Resnet50 ($\mathcal{B}3$). The table shows the Top-1 accuracy and the number of parameters.² As shown, the results demonstrate that our proposed method is comparable to the accuracy of the original model, where $h_{\{1\}}$ and $h_{\{2\}}$ refine one another, leading to improved final downstream accuracy for $h_{\{1,2\}}$. Using our approach, the individual upstream models’ accuracy is not sacrificed, ensuring that the system remains robust—if server 1 or server 2 fail, either will perform reasonably well as a failover mechanism. For instance, the table shows that upstream models can achieve up to 95.6% of ensemble accuracy in case of failures. Also, we are able to achieve this effectively with a reasonably smaller number of parameters (translates to lesser memory and computational requirements), providing an additional benefit of using this strategy.

Overall Performance. Results across a broader evaluation, as in Table 3, show that our training approach is effective in creating performant upstream and downstream models across datasets and model architectures.

²For $h_{\{1,2\}}$, the number of parameters represents the whole ensemble including exits for $h_{\{1\}}$ and $h_{\{2\}}$.

Table 3: MEL performance is evaluated across datasets and DNN models. For each model, the task-relevant performance for individual models $h_{\{1\}}$ and $h_{\{2\}}$ and their combination $h_{\{1,2\}}$ is presented. \dagger Top-1 Acc. is reported for classification tasks (CIFAR-100, TieredImageNet, Speech Commands); Word Error Rate (WER) is reported for DeepSpeech2; and Perplexity is reported for BookCorpus.

Dataset	DNN Model	MEL						Original	
		$h_{\{1\}}$		$h_{\{2\}}$		$h_{\{1,2\}}$		Perf. \dagger	Para.
		Perf. \dagger	Para.	Perf. \dagger	Para.	Perf. \dagger	Para.		
CIFAR-100	EfficientNet-B0 ($\mathcal{B}1$)	0.1883	4.08K	0.2162	4.08K	0.2365	11.45K	0.7763	4.79M
	EfficientNet-B0 ($\mathcal{B}2$)	0.4070	21.59K	0.4362	21.59K	0.4634	48.08K		
	EfficientNet-B0 ($\mathcal{B}3$)	0.5824	0.07M	0.5885	0.07M	0.6261	0.15M		
	EfficientNet-B0 ($\mathcal{B}4$)	0.6785	0.32M	0.6804	0.32M	0.7169	0.65M		
	EfficientNet-B0 ($\mathcal{B}5$)	0.7371	0.88M	0.7428	0.88M	0.7769	1.79M		
	EfficientNet-B0 ($\mathcal{B}6$)	0.7529	2.90M	0.7548	2.90M	0.7888	5.83M		
	EfficientNet-B0 ($\mathcal{B}7$)	0.7308	3.60M	0.7567	3.60M	0.7838	7.3M		
	Resnet50 ($\mathcal{B}2$)	0.6523	1.40M	0.6488	1.40M	0.6820	3.30M	0.7593	23.93M
	Resnet50 ($\mathcal{B}3$)	0.7324	8.76M	0.7043	8.76M	0.7552	17.50M		
	ViT-B/16 ($\mathcal{B}1$)	0.4644	7.80M	0.4667	7.80M	0.5066	15.90M	0.6164	85.85M
	ViT-B/16 ($\mathcal{B}2$)	0.5583	14.90M	0.5652	14.90M	0.5937	30.00M		
	ViT-B/16 ($\mathcal{B}3$)	0.5744	22.00M	0.5860	22.00M	0.6103	44.30M		
	ViT-B/16 ($\mathcal{B}4$)	0.5892	29.17M	0.5908	29.17M	0.6167	58.49M		
	ViT-B/16 ($\mathcal{B}5$)	0.5909	36.00M	0.5960	36.00M	0.6250	72.00M		
ViT-B/16 ($\mathcal{B}6$)	0.6030	43.00M	0.6034	43.00M	0.6295	86.00M			
EfficientNet-B0 ($\mathcal{B}4$)	0.6007	0.32M	0.6048	0.32M	0.6430	0.69M	0.7352		
EfficientNet-B0 ($\mathcal{B}5$)	0.6367	0.99M	0.6359	0.99M	0.6771	1.98M			
EfficientNet-B0 ($\mathcal{B}6$)	0.6957	3.11M	0.7096	3.11M	0.7420	6.22M			
Speech Commands	EfficientNet-B0 ($\mathcal{B}2$)	0.8042	0.02M	0.8224	0.02M	0.8413	0.05M	0.9638	4.05M
	EfficientNet-B0 ($\mathcal{B}3$)	0.9397	0.06M	0.9379	0.06M	0.9516	0.14M		
	EfficientNet-B0 ($\mathcal{B}4$)	0.9587	0.31M	0.9609	0.31M	0.9643	0.64M		
	EfficientNet-B0 ($\mathcal{B}5$)	0.9632	0.86M	0.9670	0.86M	0.9690	1.74M		
	EfficientNet-B0 ($\mathcal{B}6$)	0.9596	2.90M	0.9644	2.90M	0.9686	5.81M		
DeepSpeech2	DeepSpeech2 ($\mathcal{B}1$)	0.1590	7.27M	0.1660	7.27M	0.1412	14.58M	0.1046	19.89M
	DeepSpeech2 ($\mathcal{B}2$)	0.1260	10.43M	0.1270	10.43M	0.1098	20.88M		
BookCorpus	GPT-mini ($\mathcal{B}1$)	33.38	7.5M	33.38	7.5M	32.28	31.4M	23.50	33.6M
	GPT-mini ($\mathcal{B}2$)	28.16	10.5M	28.02	10.5M	27.38	37.7M		

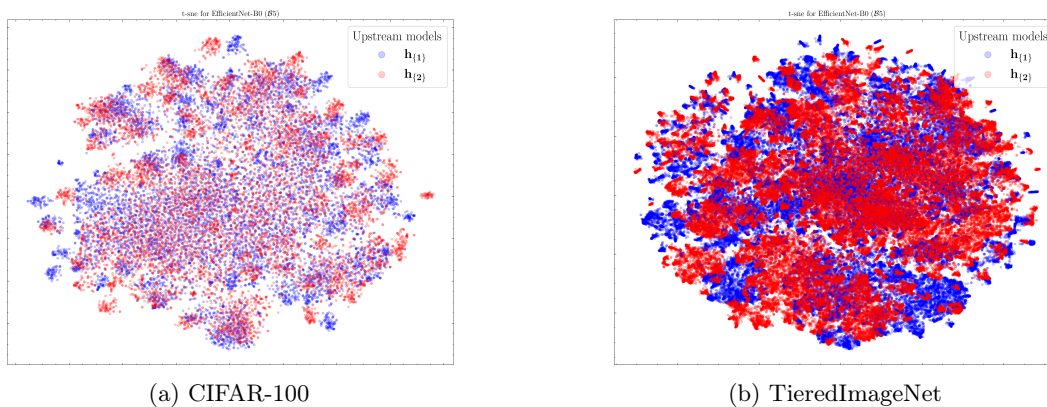


Figure 2: t-SNE visualization of features from upstream models $h_{\{1\}}$, $h_{\{2\}}$ in the MEL framework, distinguished by color, for EfficientNet-B0 ($\mathcal{B}5$) on the CIFAR-100 and TieredImageNet datasets.

The combined downstream model $h_{\{1,2\}}$ behaves similarly and sometimes *better* than the original model with a smaller parameter budget. For instance, Efficient-B0 ($\mathcal{B}3$) trained on the Mel-Spectrogram of Speech Commands dataset behaves similarly to the original model, despite only having around 15% of the parameters. In cases where we achieve the performance with a similar range of parameters when compared to the original, there is design flexibility, in the sense that the ensemble model trained using MEL approach can better utilize the same parameter budget (i.e., memory requirements), with a more resilient execution towards failures.

Feature visualization To qualitatively assess the behavior of models trained under the MEL framework, we visualize the learned feature embeddings from upstream models h_1 and h_2 using t-SNE dimensionality

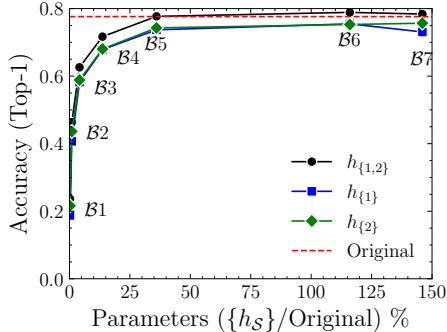


Figure 3: Effect of ensemble size of EfficientNet-B0 on CIFAR-100.

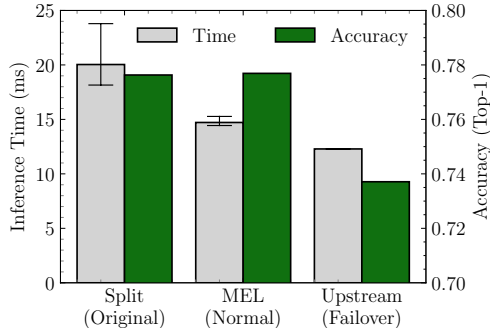


Figure 4: EfficientNet-B0 (\mathcal{B}_5) response time on CIFAR-100.

Table 4: Effect of hierarchical training and fine-tuning. Reducing task complexity improves the accuracy of *small* models ($h_{\{1\}}, h_{\{2\}}$), while fine-tuning $h_{\{1,2\}}$ provides additional gains. Note that models trained on different granularities are incomparable, as they solve slightly different problems.

Dataset	DNN Model	Fine-Grain Labels				Coarse-Grain Labels			
		$h_{\{1\}}$	$h_{\{2\}}$	$h_{\{1,2\}}$ w/o FT	$h_{\{1,2\}}$	$h_{\{1\}}$	$h_{\{2\}}$	$h_{\{1,2\}}$ w/o FT	$h_{\{1,2\}}$
CIFAR-100	EfficientNet-B0 (\mathcal{B}_4)	0.6785	0.6804	0.7147	0.7169	0.7890	0.8104	0.7188	0.7215
	EfficientNet-B0 (\mathcal{B}_5)	0.7371	0.7428	0.7765	0.7769	0.8197	0.8360	0.7610	0.7617
	Resnet50 (\mathcal{B}_3)	0.7324	0.7043	0.7512	0.7552	0.7704	0.8005	0.7402	0.7423

reduction on CIFAR-100 and TieredImageNet datasets as shown in Figure 2. As expected, there is an overlap that exists between the representations, but also the embeddings reveal that the models also capture complementary information. This indicates that during MEL training, the upstream models learn some mutually refining information/diversity among upstream models, enabling them to enhance downstream performance when combined by $h_{\{1,2\}}$ by covering different aspects of the input space.

4.3 Ablation studies

Effect of model size. DNNs are notorious for their accuracy-size trade-offs, where resource availability dictates the accuracy. Figure 3 shows the effect of the ensemble size by comparing the number of parameters in $h_{\{S\}}$ to the parameters in the *original* model on the accuracy of $h_{\{1\}}$, $h_{\{2\}}$, and $h_{\{1,2\}}$. The results highlight that as the size of the ensemble approaches 40% of the original model, \mathcal{B}_5 in this case, the performance of the MEL ensemble becomes similar to that of the original model. Moreover, the results show that increasing the number of blocks raises the total size, even surpassing the original model, with diminishing returns, highlighting considerations for users when choosing their backup models.

Hierarchical Training. As discussed in Section 3, a key design decision for the upstream models is the ability to adjust the model complexity by changing the output granularity, *i.e.* utilizing the 20 superclasses coarse labels from CIFAR-100 to train upstream models $h_{\{1\}}$, $h_{\{2\}}$, while training downstream $h_{\{1,2\}}$ on the fine labels of the dataset. The effect of such a learning procedure is shown in Table 4. Notably, the smaller backup models have 83.6% accuracy, attributed to the fact that the subproblem is less complex, and the ensemble accuracy is still maintained on the fine-label classes.

Finetuning. Table 4 depicts the effect of the additional fine-tuning on the downstream model while freezing the weights of the upstream models. The results show that the fine-tuning step is more beneficial in a hierarchical learning design, as in the case of EfficientNet-B0 (\mathcal{B}_4), increasing the accuracy from 71.88% to 72.15%.

Downstream model architecture. Table 5 compares the accuracy of MEL across different downstream model architectures. We focus on two architectures for the downstream models, fully connected networks (FC) and convolutional neural networks (CNNs), and test different sizes. The results show that *using different architectures for the downstream models can optimize the ensemble accuracy with little to no effect on the upstream models*. The table also shows that increasing the size of the FC networks by adding hidden layers

Table 5: Comparison of different downstream architectures in MEL for combining upstream outputs. FC (None) uses only a classification layer; FC (256) adds a dense layer with 256 units. CNN (160) and CNN (320) include convolutional layers with the specified number of channels before classification.

Dataset	DNN Model	Downstream Model (Size)	MEL			Total Size
			$h_{\{1\}}$	$h_{\{2\}}$	$h_{\{1,2\}}$	
CIFAR-100	EfficientNet-B0 ($\mathcal{B}5$)	FC (None)	0.7371	0.7428	0.7769	1.79M
		FC (256)	0.7224	0.7412	0.7610	1.81M
		CNN (160)	0.7156	0.7523	0.7743	1.79M
		CNN (320)	0.7451	0.7467	0.7810	1.83M
	Resnet50 ($\mathcal{B}3$)	FC (None)	0.7324	0.70432	0.7552	17.50M
		FC (256)	0.7113	0.7252	0.6931	17.84M
		CNN (160)	0.7060	0.7223	0.7483	17.64M
		CNN (320)	0.7058	0.7161	0.7557	17.98M
TieredImageNet	EfficientNet-B0 ($\mathcal{B}5$)	FC (None)	0.6367	0.6359	0.6771	1.98M
		FC (256)	0.6492	0.6560	0.6713	2.05M
		CNN (160)	0.6574	0.6595	0.6873	1.98M
		CNN (320)	0.6618	0.6665	0.7022	2.11M

Table 6: Impact of varying weights on the upstream vs downstream models during MEL training with EfficientNet-B0 ($\mathcal{B}5$) on CIFAR-100. λ_1 corresponds to the weight of the upstream models (*i.e.* $h_{\{1\}}$, $h_{\{2\}}$), while λ_{12} controls the weight of the downstream model $h_{\{1,2\}}$ in the loss formulation. Top-1 accuracy is reported across the different downstream head architectures. We omit the fine-tuning step to show the effect of weights on the accuracy of all models.

Downstream Model (Size)	$\lambda_1 : \lambda_{12}$	MEL		
		$h_{\{1\}}$	$h_{\{2\}}$	$h_{\{1,2\}}$
FC (None)	1 : 5	0.6317	0.7325	0.7631
	1 : 2	0.7064	0.7484	0.7735
	1 : 1	0.7371	0.7428	0.7769
	2 : 1	0.7267	0.7522	0.7754
	5 : 1	0.7515	0.7528	0.7787
FC (256)	1 : 5	0.5687	0.7238	0.7479
	1 : 2	0.7164	0.7458	0.7665
	1 : 1	0.7224	0.7412	0.7610
	2 : 1	0.7464	0.7631	0.7840
	5 : 1	0.7536	0.7654	0.7852
CNN (160)	1 : 5	0.6629	0.7391	0.7764
	1 : 2	0.6986	0.7617	0.7825
	1 : 1	0.7156	0.7573	0.7743
	2 : 1	0.7571	0.7661	0.7882
	5 : 1	0.7611	0.7625	0.7832
CNN (320)	1 : 5	0.6966	0.7032	0.7735
	1 : 2	0.7325	0.7493	0.7814
	1 : 1	0.7451	0.7467	0.7810
	2 : 1	0.7602	0.7609	0.7917
	5 : 1	0.7600	0.7625	0.7883

typically does not increase the accuracy. For instance, going from a concatenation layer and a classification layer (*i.e.*, FC (None)) to adding a hidden layer with 256 neurons did not enhance the accuracy. We note that this issue can be resolved by using higher weights for the upstream models (see Table 5). In contrast, increasing the size of CNNs (*i.e.*, by adding more filters) typically increases the accuracy. Similarly, we note that higher weights for the upstream models can further enhance the accuracy (see Table 5).

Effect of relative importance. Table 6 presents the effect of varying the relative importance of upstream and downstream models during MEL training with EfficientNet-B0 ($\mathcal{B}5$) on CIFAR-100, across different downstream head architectures and configurations. The results indicate that *increasing the upstream model’s relative importance (i.e. more λ_1 and λ_2 as compared to λ_{12}) typically improves overall accuracy*. For example, assigning a 2:1 weight in favor of the upstream models with the CNN (320) head yields a $1.82\times$ improvement in downstream accuracy, while also enhancing the performance of the individual upstream models.

Table 7: Performance of individual backup models $h_{\{1\}}$, $h_{\{2\}}$ under joint optimization within the MEL framework compared to individual training.

Dataset	DNN Model	MEL Perf.		Standalone
		$h_{\{1\}}$	$h_{\{2\}}$	
CIFAR-100	EfficientNet-B0 ($\mathcal{B}1$)	0.1883	0.2162	0.2060
	EfficientNet-B0 ($\mathcal{B}2$)	0.4070	0.4362	0.4268
	EfficientNet-B0 ($\mathcal{B}3$)	0.5824	0.5885	0.5809
	EfficientNet-B0 ($\mathcal{B}4$)	0.6785	0.6804	0.7105
	EfficientNet-B0 ($\mathcal{B}5$)	0.7428	0.7371	0.7471
	EfficientNet-B0 ($\mathcal{B}6$)	0.7529	0.7548	0.7686
	Resnet50 ($\mathcal{B}2$)	0.6523	0.6488	0.6801
	Resnet50 ($\mathcal{B}3$)	0.7324	0.7043	0.7263
	ViT-B/16 ($\mathcal{B}1$)	0.4644	0.4667	0.4740
	ViT-B/16 ($\mathcal{B}2$)	0.5583	0.5652	0.5685
	ViT-B/16 ($\mathcal{B}3$)	0.5744	0.5860	0.5916
	ViT-B/16 ($\mathcal{B}4$)	0.5892	0.5908	0.6013
ViT-B/16 ($\mathcal{B}5$)	0.5909	0.5960	0.6044	
ViT-B/16 ($\mathcal{B}6$)	0.6030	0.6034	0.6100	
Tiered-Imagenet	EfficientNet-B0 ($\mathcal{B}4$)	0.6007	0.6048	0.5847
	EfficientNet-B0 ($\mathcal{B}5$)	0.6367	0.6359	0.6555
	EfficientNet-B0 ($\mathcal{B}6$)	0.6957	0.7096	0.6905
Speech Commands	EfficientNet-B0 ($\mathcal{B}2$)	0.8042	0.8224	0.8134
	EfficientNet-B0 ($\mathcal{B}3$)	0.9397	0.9379	0.9421
	EfficientNet-B0 ($\mathcal{B}4$)	0.9587	0.9609	0.9625
	DeepSpeech2 ($\mathcal{B}1$)	0.1590	0.1660	0.1520
	DeepSpeech2 ($\mathcal{B}2$)	0.1260	0.1270	0.1185
BookCorpus	GPT-mini ($\mathcal{B}1$)	33.38	33.38	33.41
	GPT-mini ($\mathcal{B}2$)	28.16	28.02	28.67

4.4 Comparing to Baselines

In this section, we evaluate the performance of MEL in comparison with the baselines as outlined in Section 4.1. In addition to the original and small failover replica configurations, we introduce the *individual* and *standalone* baselines to explore different effects in these other natural alternatives to MEL, as prior work is limited in addressing this specific problem setting.

Single failover replicas. Reasonably, we expect our upstream models $h_{\{1\}}$ and $h_{\{2\}}$ trained within the ensemble strategy to be as competitive as traditional compressed models. Table 7 draws this comparison among architectures and datasets between upstream models and a *small* model of the same size trained in isolation, to mimic typical compact backup replicas. The results show that these models trained within the ensemble have proximate behaviors to their independently trained counterparts, which demonstrates the effectiveness of our training methodology in not compromising the individual effectiveness of the upstream backup models.

Training strategies. Table 8 shows the performance of h_S architecture trained using our proposed MEL ensembling approach against previously discussed baselines — **standalone** (trained as a whole for one downstream accuracy), and the **individually-trained** ensemble (i.e., upstream and downstream models are trained in two stages). In almost all cases, the results show that our ensembling approach yields the highest accuracy compared to the baselines, where the results show that our training strategy allows the models to achieve resiliency by operating as smaller models while maintaining the accuracy of a standalone model, trained on a single objective. More importantly, although the individually trained models also offer resilience, our MEL ensembles consistently achieve higher performance, highlighting the benefits of MEL that produces mutually refining upstream models. Additional comprehensive evaluation will also be available in Appendix F.

4.5 System Evaluation

Figure 4 shows the response time when deploying our architecture on three Nvidia A2 GPUs. We compare the accuracy and inference time of our MEL based on EfficientNet-B0 ($\mathcal{B}5$) in the normal operation mode (i.e., all three servers are available), and a scenario where only an upstream model is available. For comparison, use a split inference approach [33] running the original models, where the model is split ($\mathcal{B}1$ -5, $\mathcal{B}6$, and

Table 8: Performance of $h_{\{1,2\}}$ under different training strategies –Standalone trains only $h_{\{1,2\}}$, while Individually trained trains $h_{\{1\}}, h_{\{2\}}$ independently and then optimizes $h_{\{1,2\}}$ with frozen upstream models.

Dataset	DNN Model	MEL Perf.	Standalone	Ind. Trained
CIFAR-100	EfficientNet-B0 ($\mathcal{B}1$)	0.2365	0.2523	0.2086
	EfficientNet-B0 ($\mathcal{B}2$)	0.4634	0.4662	0.4155
	EfficientNet-B0 ($\mathcal{B}3$)	0.6261	0.6181	0.6072
	EfficientNet-B0 ($\mathcal{B}4$)	0.7169	0.7064	0.7038
	EfficientNet-B0 ($\mathcal{B}5$)	0.7769	0.7524	0.7462
	EfficientNet-B0 ($\mathcal{B}6$)	0.7888	0.7662	0.7615
	Resnet50 ($\mathcal{B}2$)	0.6801	0.6338	0.6593
	Resnet50 ($\mathcal{B}3$)	0.7552	0.7579	0.7235
	ViT-B/16 ($\mathcal{B}1$)	0.5066	0.5008	0.4829
	ViT-B/16 ($\mathcal{B}2$)	0.5937	0.5874	0.5720
	ViT-B/16 ($\mathcal{B}3$)	0.6103	0.6160	0.5947
	ViT-B/16 ($\mathcal{B}4$)	0.6167	0.6111	0.6001
	ViT-B/16 ($\mathcal{B}5$)	0.6250	0.6279	0.6071
	ViT-B/16 ($\mathcal{B}6$)	0.6295	0.6149	0.6126
Tiered-Imagenet	EfficientNet-B0 ($\mathcal{B}5$)	0.6430	0.6365	0.5905
	EfficientNet-B0 ($\mathcal{B}5$)	0.6771	0.6955	0.6589
	EfficientNet-B0 ($\mathcal{B}6$)	0.7420	0.7207	0.6925
Speech Commands	EfficientNet-B0 ($\mathcal{B}2$)	0.8413	0.8495	0.8206
	EfficientNet-B0 ($\mathcal{B}3$)	0.9516	0.9504	0.9457
	EfficientNet-B0 ($\mathcal{B}4$)	0.9643	0.9623	0.9634
	DeepSpeech2 ($\mathcal{B}1$)	0.1412	0.1546	0.1499
	DeepSpeech2 ($\mathcal{B}2$)	0.1098	0.1217	0.1181
Bookcorpus	GPT-mini ($\mathcal{B}1$)	32.28	28.99	33.04
	GPT-mini ($\mathcal{B}2$)	27.38	25.21	28.15

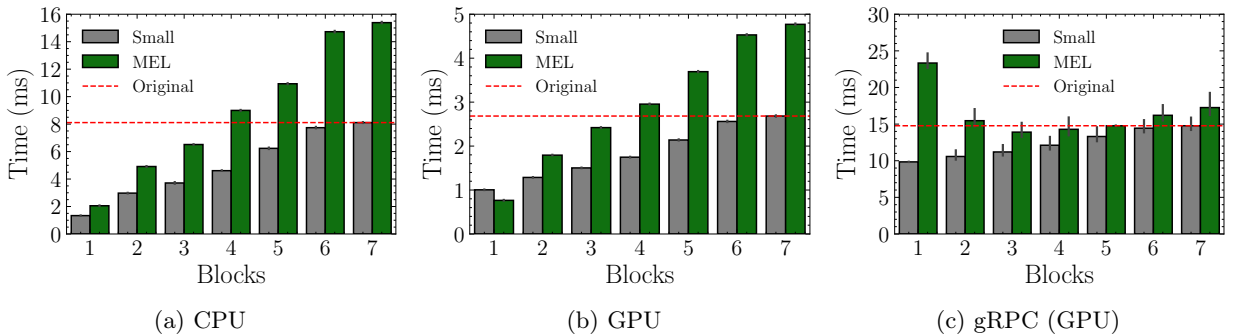


Figure 5: Processing Latency of EfficientNet-B0 on CIFAR-100.

$\mathcal{B}7$ /Classifier). As shown, our approach demonstrates a lower inference time than a typical split model, as we are able to parallelize the execution of the two models by placing them on different servers, yielding a 25% improvement in response time.

We also evaluate the performance of the proposed ensemble models on both CPU and GPU, when deployed on single server for EfficientNet-B0, as in Figure 5. As one would expect, increasing the number of blocks increases latency — moving from 1 to 5 blocks increases latency by 4.8ms and 8.9ms for the standalone and MEL models, respectively due to the fact that ensemble models are wider and require more computation. However, there is also more important aspect that when deployed across multiple servers (*i.e.* in the intended setup), the results demonstrate that while using a smaller sub-blocks configuration may have lower parameter count, they might yield a higher response times – consistent with prior split processing work [20]. Once past the initial layers, performance stabilizes, and MEL introduces only minimal overhead. We expand our evaluation across scenarios in Appendix G.

5 Conclusion

In this paper, we presented our Multi-level Ensemble Learning (MEL) approach for resilient edge inference and experimentally demonstrated its efficacy through extensive evaluation. By training ensemble backup models

under joint optimization, it is able to take advantage of the fact that when multiple models succeed, the performance is mutually refined. Our work has a few limitations. First, in scenarios where edge resources are heterogeneous or utilized unevenly, the upstream models may need to be heterogeneous themselves (in terms of size), an aspect which we did not study. Secondly, the question of choosing the optimal configuration from a family of MEL models that we trained is not explored in this work. Both limitations are also opportunities for future work. In terms of broader impact, our work promises a foundation for a robust edge AI to become more prevalent in the future and enable a new generation of resilient, latency-sensitive inference applications such as AR, personal robotics, and more.

References

- [1] Sohaib Ahmad, Hui Guan, Brian D. Friedman, Thomas Williams, Ramesh K. Sitaraman, and Thomas Woo. Proteus: A High-Throughput Inference-Serving System with Accuracy Scaling. In *Proceedings of the 29th ACM International Conference on Architectural Support for Programming Languages and Operating Systems, Volume 1*, ASPLOS '24, page 318–334, New York, NY, USA, 2024. Association for Computing Machinery.
- [2] Sohaib Ahmad, Hui Guan, and Ramesh K. Sitaraman. Loki: A System for Serving ML Inference Pipelines with Hardware and Accuracy Scaling. In *Proceedings of the 33rd International Symposium on High-Performance Parallel and Distributed Computing*, HPDC '24, page 267–280, New York, NY, USA, 2024. Association for Computing Machinery.
- [3] Dario Amodei, Rishita Anubhai, Eric Battenberg, Carl Case, Jared Casper, Bryan Catanzaro, Jingdong Chen, Mike Chrzanowski, Adam Coates, Greg Diamos, Erich Elsen, Jesse Engel, Linxi Fan, Christopher Fougner, Tony Han, Awni Hannun, Billy Jun, Patrick LeGresley, Libby Lin, Sharan Narang, Andrew Ng, Sherjil Ozair, Ryan Prenger, Jonathan Raiman, Sanjeev Satheesh, David Seetapun, Shubho Sengupta, Yi Wang, Zhiqian Wang, Chong Wang, Bo Xiao, Dani Yogatama, Jun Zhan, and Zhenyao Zhu. Deep speech 2: End-to-end speech recognition in english and mandarin, 2015.
- [4] Amin Banitalebi-Dehkordi, Naveen Vedula, Jian Pei, Fei Xia, Lanjun Wang, and Yong Zhang. Auto-Split: A General Framework of Collaborative Edge-Cloud AI. In *Proceedings of the 27th ACM SIGKDD Conference on Knowledge Discovery & Data Mining*, KDD '21, page 2543–2553, New York, NY, USA, 2021. Association for Computing Machinery.
- [5] Leo Breiman. Bagging predictors. *Machine learning*, 24:123–140, 1996.
- [6] Leo Breiman. Random forests. *Machine learning*, 45:5–32, 2001.
- [7] Yuheng Bu, Weihao Gao, Shaofeng Zou, and Venugopal Veeravalli. Information-theoretic understanding of population risk improvement with model compression. In *Proceedings of the AAAI Conference on Artificial Intelligence*, volume 34, pages 3300–3307, 2020.
- [8] Tianqi Chen, Thierry Moreau, Ziheng Jiang, Lianmin Zheng, Eddie Yan, Meghan Cowan, Haichen Shen, Leyuan Wang, Yuwei Hu, Luis Ceze, Carlos Guestrin, and Arvind Krishnamurthy. Tvm: an automated end-to-end optimizing compiler for deep learning. In *Proceedings of the 13th USENIX Conference on Operating Systems Design and Implementation*, OSDI'18, page 579–594, USA, 2018. USENIX Association.
- [9] Daniel Crankshaw, Xin Wang, Guilio Zhou, Michael J. Franklin, Joseph E. Gonzalez, and Ion Stoica. Clipper: A Low-Latency online prediction serving system. In *14th USENIX Symposium on Networked Systems Design and Implementation (NSDI 17)*, pages 613–627, Boston, MA, March 2017. USENIX Association.
- [10] Jia Deng, Wei Dong, Richard Socher, Li-Jia Li, Kai Li, and Li Fei-Fei. ImageNet: A large-scale hierarchical image database. In *2009 IEEE Conference on Computer Vision and Pattern Recognition*, pages 248–255, 2009.
- [11] Alexey Dosovitskiy, Lucas Beyer, Alexander Kolesnikov, Dirk Weissenborn, Xiaohua Zhai, Thomas Unterthiner, Mostafa Dehghani, Matthias Minderer, Georg Heigold, Sylvain Gelly, Jakob Uszkoreit, and Neil Houlsby. An Image is Worth 16x16 Words: Transformers for Image Recognition at Scale, 2021.
- [12] Yoav Freund and Robert E Schapire. A decision-theoretic generalization of on-line learning and an application to boosting. *Journal of computer and system sciences*, 55(1):119–139, 1997.
- [13] Arpan Gujarati, Reza Karimi, Safya Alzayat, Wei Hao, Antoine Kaufmann, Ymir Vigfusson, and Jonathan Mace. Serving DNNs like clockwork: Performance predictability from the bottom up. In *14th USENIX Symposium on Operating Systems Design and Implementation (OSDI 20)*, pages 443–462. USENIX Association, November 2020.

- [14] Mahdi Haghifam, Jeffrey Negrea, Ashish Khisti, Daniel M Roy, and Gintare Karolina Dziugaite. Sharpened generalization bounds based on conditional mutual information and an application to noisy, iterative algorithms. In *Advances in Neural Information Processing Systems*, volume 33, pages 9925–9935. Curran Associates, Inc., 2020.
- [15] Walid A. Hanafy, Tergel Molom-Ochir, and Rohan Shenoy. Design Considerations for Energy-Efficient Inference on Edge Devices. In *Proceedings of the Twelfth ACM International Conference on Future Energy Systems*, e-Energy '21, page 302–308, New York, NY, USA, 2021. Association for Computing Machinery.
- [16] Walid A. Hanafy, Limin Wang, Hyunseok Chang, Sarit Mukherjee, T. V. Lakshman, and Prashant Shenoy. Understanding the Benefits of Hardware-Accelerated Communication in Model-Serving Applications. In *2023 IEEE/ACM 31st International Symposium on Quality of Service (IWQoS)*, pages 1–10, 2023.
- [17] Walid A. Hanafy, Li Wu, Tarek Abdelzaher, Suhas Diggavi, and Prashant Shenoy. Failure-Resilient ML Inference at the Edge through Graceful Service Degradation. In *MILCOM 2023 - 2023 IEEE Military Communications Conference (MILCOM)*, pages 144–149, 2023.
- [18] Hrayr Harutyunyan, Maxim Raginsky, Greg Ver Steeg, and Aram Galstyan. Information-theoretic generalization bounds for black-box learning algorithms. In *Advances in Neural Information Processing Systems*, volume 34, pages 24670–24682. Curran Associates, Inc., 2021.
- [19] Kaiming He, Xiangyu Zhang, Shaoqing Ren, and Jian Sun. Deep Residual Learning for Image Recognition. In *Proceedings of the IEEE conference on computer vision and pattern recognition (CVPR)*, 2016.
- [20] Jin Huang, Colin Samplawski, Deepak Ganesan, Benjamin Marlin, and Heesung Kwon. CLIO: Enabling Automatic Compilation of Deep Learning Pipelines across IoT and Cloud. In *Proceedings of the 26th Annual International Conference on Mobile Computing and Networking*, MobiCom '20, New York, NY, USA, 2020. Association for Computing Machinery.
- [21] Daniel Jakubovitz, Raja Giryes, and Miguel RD Rodrigues. Generalization error in deep learning. In *Compressed sensing and its applications: third international MATHEOn conference 2017*, pages 153–193. Springer, 2019.
- [22] Michael I Jordan and Robert A Jacobs. Hierarchical mixtures of experts and the em algorithm. *Neural computation*, 6(2):181–214, 1994.
- [23] Israel Koren and C. Mani Krishna. *Fault-Tolerant Systems*. Morgan Kaufmann, second edition edition, 2021.
- [24] Alex Krizhevsky. Learning Multiple Layers of Features from Tiny Images. Technical report, University of Toronto, 2009. Technical Report.
- [25] Kubeflow. Kubeflow: The machine learning toolkit for kubernetes, 2025. Accessed: 2025-04-14.
- [26] En Li, Liekang Zeng, Zhi Zhou, and Xu Chen. Edge ai: On-demand accelerating deep neural network inference via edge computing. *IEEE Transactions on Wireless Communications*, 19(1):447–457, 2020.
- [27] Qianlin Liang, Walid A. Hanafy, Ahmed Ali-Eldin, and Prashant Shenoy. Model-Driven Cluster Resource Management for AI Workloads in Edge Clouds. *ACM Trans. Auton. Adapt. Syst.*, 18(1), mar 2023.
- [28] Qianlin Liang, Walid A. Hanafy, Noman Bashir, Ahmed Ali-Eldin, David Irwin, and Prashant Shenoy. DeLen: Enabling Flexible and Adaptive Model-Serving for Multi-Tenant Edge AI. In *Proceedings of the 8th ACM/IEEE Conference on Internet of Things Design and Implementation*, IoTDI '23, page 209–221, New York, NY, USA, 2023. Association for Computing Machinery.
- [29] Qianlin Liang, Prashant Shenoy, and David Irwin. AI on the Edge: Characterizing AI-based IoT Applications Using Specialized Edge Architectures. In *2020 IEEE International Symposium on Workload Characterization (IISWC)*, pages 145–156, 2020.
- [30] Ilya Loshchilov and Frank Hutter. SGDR: Stochastic Gradient Descent with Warm Restarts, 2017.
- [31] Ilya Loshchilov and Frank Hutter. Decoupled Weight Decay Regularization, 2019.
- [32] Ayesha Abdul Majeed, Peter Kilpatrick, Ivor Spence, and Blesson Varghese. Continuer: maintaining distributed dnn services during edge failures. In *2022 IEEE International Conference on Edge Computing and Communications (EDGE)*, pages 143–152. IEEE, 2022.
- [33] Yoshitomo Matsubara, Marco Levorato, and Francesco Restuccia. Split computing and early exiting for deep learning applications: Survey and research challenges. *ACM Comput. Surv.*, 55(5), December 2022.

- [34] Justin J. Meza, Thote Gowda, Ahmed Eid, Tomiwa Ijaware, Dmitry Chernyshev, Yi Yu, Md Nazim Uddin, Rohan Das, Chad Nachiappan, Sari Tran, Shuyang Shi, Tina Luo, David Ke Hong, Sankaralingam Panneerselvam, Hans Ragas, Svetlin Manavski, Weidong Wang, and Francois Richard. Defcon: Preventing Overload with Graceful Feature Degradation. In *17th USENIX Symposium on Operating Systems Design and Implementation (OSDI 23)*, pages 607–622, Boston, MA, July 2023. USENIX Association.
- [35] Microsoft Corp. ONNX Runtime. <https://onnxruntime.ai/>, 2025. Accessed: 2025-05-20.
- [36] NVIDIA. Triton inference server, 2024. Accessed: 2025-04-13.
- [37] Christopher Olston, Noah Fiedel, Kiril Gorovoy, Jeremiah Harmsen, Li Lao, Fangwei Li, Vinu Rajashekhara, Sukriti Ramesh, and Jordan Soyke. Tensorflow-serving: Flexible, high-performance ml serving. *arXiv preprint arXiv:1712.06139*, 2017.
- [38] Mohamad Rida Rammal, Alessandro Achille, Aditya Golatkar, Suhas N. Diggavi, and Stefano Soatto. On leave-one-out conditional mutual information for generalization. In *Advances in Neural Information Processing Systems NeurIPS*, 2022.
- [39] Mengye Ren, Eleni Triantafillou, Sachin Ravi, Jake Snell, Kevin Swersky, Joshua B. Tenenbaum, Hugo Larochelle, and Richard S. Zemel. Meta-Learning for Semi-Supervised Few-Shot Classification. In *Proceedings of 6th International Conference on Learning Representations ICLR*, 2018.
- [40] Daniel Russo and James Zou. Controlling bias in adaptive data analysis using information theory. In *Proceedings of the 19th International Conference on Artificial Intelligence and Statistics*, volume 51 of *Proceedings of Machine Learning Research*, pages 1232–1240, Cadiz, Spain, 09–11 May 2016. PMLR.
- [41] Colin Samplawski, Jin Huang, Deepak Ganesan, and Benjamin M. Marlin. Towards objection detection under iot resource constraints: Combining partitioning, slicing and compression. In *Proceedings of the 2nd International Workshop on Challenges in Artificial Intelligence and Machine Learning for Internet of Things*, AIChallengeIoT '20, page 14–20, New York, NY, USA, 2020. Association for Computing Machinery.
- [42] Colin Samplawski, Jin Huang, Deepak Ganesan, and Benjamin M. Marlin. Towards objection detection under iot resource constraints: Combining partitioning, slicing and compression. In *Proceedings of the 2nd International Workshop on Challenges in Artificial Intelligence and Machine Learning for Internet of Things*, AIChallengeIoT '20, page 14–20, New York, NY, USA, 2020. Association for Computing Machinery.
- [43] Mahadev Satyanarayanan. The Emergence of Edge Computing. *Computer*, 50(1):30–39, 2017.
- [44] Mahadev Satyanarayanan, Nathan Beckmann, Grace A. Lewis, and Brandon Lucia. The Role of Edge Offload for Hardware-Accelerated Mobile Devices. In *Proceedings of the 22nd International Workshop on Mobile Computing Systems and Applications*, HotMobile '21, page 22–29, New York, NY, USA, 2021. Association for Computing Machinery.
- [45] Simone Scardapane, Michele Scarpiniti, Enzo Baccarelli, and Aurelio Uncini. Why Should We Add Early Exits to Neural Networks? *Cognitive Computation*, 12(5):954–966, 2020.
- [46] Shai Shalev-Shwartz and Shai Ben-David. *Understanding Machine Learning: From Theory to Algorithms*. Cambridge University Press, USA, 2014.
- [47] Noam Shazeer, Azalia Mirhoseini, Krzysztof Maziarz, Andy Davis, Quoc Le, Geoffrey Hinton, and Jeff Dean. Outrageously large neural networks: The sparsely-gated mixture-of-experts layer. In *International Conference on Learning Representations*, 2017.
- [48] Jonathan Soifer, Jason Li, Mingqin Li, Jeffrey Zhu, Yingnan Li, Yuxiong He, Elton Zheng, Adi Oltean, Maya Mosyak, Chris Barnes, Thomas Liu, and Junhua Wang. Deep Learning Inference Service at Microsoft. In *2019 USENIX Conference on Operational Machine Learning (OpML 19)*, pages 15–17, Santa Clara, CA, may 2019.
- [49] Thomas Steinke and Lydia Zakyntinou. Reasoning About Generalization via Conditional Mutual Information. In *Proceedings of Thirty Third Conference on Learning Theory*, volume 125 of *Proceedings of Machine Learning Research*, pages 3437–3452. PMLR, 09–12 Jul 2020.
- [50] Mingxing Tan and Quoc Le. EfficientNet: Rethinking Model Scaling for Convolutional Neural Networks. In *Proceedings of the 36th International Conference on Machine Learning*, volume 97 of *Proceedings of Machine Learning Research*, pages 6105–6114. PMLR, 09–15 Jun 2019.
- [51] Surat Teerapittayanon, Bradley McDanel, and H.T. Kung. Branchynet: Fast inference via early exiting from deep neural networks. In *2016 23rd International Conference on Pattern Recognition (ICPR)*, pages 2464–2469, 2016.

- [52] Chengcheng Wan, Muhammad Santriaji, Eri Rogers, Henry Hoffmann, Michael Maire, and Shan Lu. ALERT: Accurate learning for energy and timeliness. In *2020 USENIX Annual Technical Conference (USENIX ATC 20)*, pages 353–369. USENIX Association, July 2020.
- [53] P. Warden. Speech Commands: A Dataset for Limited-Vocabulary Speech Recognition. *ArXiv e-prints*, April 2018.
- [54] Ross Wightman. PyTorch Image Models. <https://github.com/huggingface/pytorch-image-models>, 2019.
- [55] Li Wu, Walid A. Hanafy, Tarek Abdelzaher, David Irwin, Jesse Milzman, and Prashant Shenoy. FailLite: Failure-Resilient Model Serving for Resource-Constrained Edge Environments, 2025.
- [56] Aolin Xu and Maxim Raginsky. Information-theoretic analysis of generalization capability of learning algorithms. *Advances in neural information processing systems*, 30, 2017.
- [57] Ashkan Yousefpour, Siddhartha Devic, Brian Q Nguyen, Aboudy Kreidieh, Alan Liao, Alexandre M Bayen, and Jason P Jue. Guardians of the deep fog: Failure-resilient dnn inference from edge to cloud. In *Proceedings of the first international workshop on challenges in artificial intelligence and machine learning for internet of things*, pages 25–31, 2019.
- [58] Ashkan Yousefpour, Brian Q Nguyen, Siddhartha Devic, Guanhua Wang, Aboudy Kreidieh, Hans Lobel, Alexandre M Bayen, and Jason P Jue. Resilinet: Failure-resilient inference in distributed neural networks. *arXiv preprint arXiv:2002.07386*, 2020.
- [59] Chengliang Zhang, Minchen Yu, wei wang, and Feng Yan. Enabling Cost-Effective, SLO-Aware Machine Learning Inference Serving on Public Cloud. *IEEE Transactions on Cloud Computing*, pages 1–1, 2020.
- [60] Jeff Zhang, Sameh Elnikety, Shuayb Zarar, Atul Gupta, and Siddharth Garg. Model-Switching: Dealing with fluctuating workloads in Machine-Learning-as-a-Service systems. In *12th USENIX Workshop on Hot Topics in Cloud Computing (HotCloud 20)*. USENIX Association, July 2020.
- [61] Shuai Zhang, Sheng Zhang, Zhuzhong Qian, Jie Wu, Yibo Jin, and Sanglu Lu. DeepSlicing: Collaborative and Adaptive CNN Inference With Low Latency. *IEEE Transactions on Parallel and Distributed Systems*, 32(9):2175–2187, 2021.
- [62] Wuyang Zhang, Sugang Li, Luyang Liu, Zhenhua Jia, Yanyong Zhang, and Dipankar Raychaudhuri. Hetero-Edge: Orchestration of Real-time Vision Applications on Heterogeneous Edge Clouds. In *IEEE INFOCOM 2019 - IEEE Conference on Computer Communications*, pages 1270–1278, 2019.
- [63] Yukun Zhu, Ryan Kiros, Rich Zemel, Ruslan Salakhutdinov, Raquel Urtasun, Antonio Torralba, and Sanja Fidler. Aligning Books and Movies: Towards Story-Like Visual Explanations by Watching Movies and Reading Books. In *The IEEE International Conference on Computer Vision (ICCV)*, December 2015.
- [64] Jie Zou, Xiaotian Dai, and John Mcdermid. Graceful Degradation with Condition- and Inference-Awareness for Mixed-Criticality Scheduling in Autonomous Systems. In *Proceedings of Cyber-Physical Systems and Internet of Things Week 2023, CPS-IoT Week '23*, page 215–220, New York, NY, USA, 2023. Association for Computing Machinery.

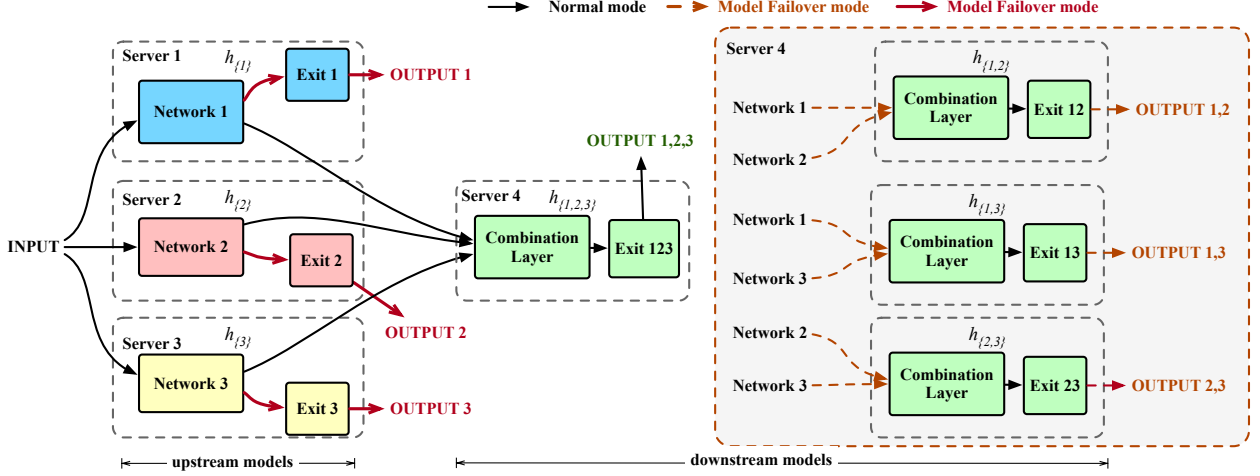


Figure 6: An example *multi-level ensemble* architecture featuring three upstream models. The figure highlights that three upstream models require four downstream models: A downstream model for the normal model, where all three models are available, and three models for different failure scenarios. Lastly, the figure highlights that models can also have their own exits in case only one server is available.

Appendix

The appendix of this paper is structured as follows.

- [Appendix A](#) presents the proof of Proposition 2.1.
- [Appendix B](#) presents the system design and implementation.
- [Appendix C](#) lists the details of the utilized datasets, model architecture, and computing resources.
- [Appendix D](#) expands the results of MEL across models and architectures.
- [Appendix E](#) expands the ablation studies of MEL across more upstream tasks, downstream architectures, and weights.
- [Appendix F](#) expands the baseline comparisons for MEL.
- [Appendix G](#) expands the performance evaluation comparisons for MEL.
- [Appendix H](#) presents the limitations of MEL.

A Proof of Proposition 2.1

Proof. We consider overall generalization error $\text{gen}_{overall}^2 = \mathbb{E}_{\mathcal{D}, h_{\{1\}}, h_{\{2\}}, h_{\{1,2\}}} [L(h_{\{1,2\}}, h_{\{1\}}, h_{\{2\}})] = \mathbb{E}[\frac{1-p}{1+p}(L(h_{\{1,2\}}) - \hat{L}(h_{\{1,2\}}))^2 + \frac{p}{1+p}(L(h_{\{1\}}) - \hat{L}(h_{\{1\}}))^2 + \frac{p}{1+p}(L(h_{\{2\}}) - \hat{L}(h_{\{2\}}))^2]$, where $0 \leq p \leq 1$ acts as a failover probability, i.e. when $p = 1$ it is guaranteed to use a lightweight model, and $p = 0$ it is guaranteed to use the ensemble model. Note that the overall generalization error (sum of squares) yields,

$$\text{gen}_{overall}^2 \leq \frac{1-p}{1+p} \frac{2\sigma^2}{n} I(\mathcal{D}; h_{\{1,2\}}) + \frac{p}{1+p} \frac{2\sigma^2}{n} (I(\mathcal{D}; h_{\{1\}}) + I(\mathcal{D}; h_{\{2\}}))$$

Using the above Markov chain and data processing inequality, we can show,

$$I(\mathcal{D}; h_{\{1,2\}}) \leq I(\mathcal{D}; h_{\{1\}}, h_{\{2\}}) = I(\mathcal{D}; h_{\{1\}}) + I(\mathcal{D}; h_{\{2\}}) - I(h_{\{1\}}, h_{\{2\}}), \quad (5)$$

where we used the following identities given the conditional independence,

$$\begin{aligned} I(\mathcal{D}; h_{\{1\}}, h_{\{2\}}) &= H(h_{\{1\}}, h_{\{2\}}) - H(h_{\{1\}}, h_{\{2\}}|D) \\ &= [H(h_{\{1\}}) + H(h_{\{2\}}) - I(h_{\{1\}}; h_{\{1,2\}})] - [H(h_{\{1\}}|D) + H(h_{\{2\}}|D)] \\ &= [H(h_{\{1\}}) - H(h_{\{1\}}|D)] + [H(h_{\{2\}}) - H(h_{\{2\}}|D)] - I(h_{\{1\}}; h_{\{2\}}) \end{aligned}$$

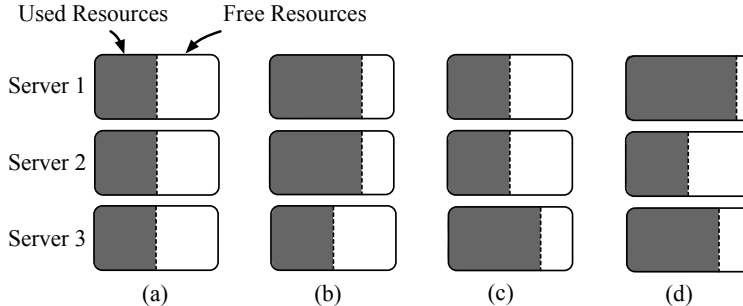


Figure 7: Resource fragmentation scenarios, where servers have equal available resources (a), and scenarios where one of the servers has more capacity than the others (b), and a scenario where one of the servers is more limited than the others (c), and (d) a scenario where all servers have different amount of resources.

$$= I(D; h_{\{1\}}) + I(D; h_{\{2\}}) - I(h_{\{1\}}; h_{\{2\}}).$$

As a result, we have,

$$\text{gen}_{overall}^2 \leq \frac{1}{1+p} \frac{2\sigma^2}{n} ((I(D; h_{\{1\}}) + I(D; h_{\{2\}})) - (1-p)(I(h_{\{1\}}; h_{\{2\}})))$$

□

B System Design and Implementation

Although model selection has been extensively studied [2, 1, 15, 55, 52], none of the previous approaches have considered selection for model ensembles. To instantiate an ensemble model, as stated in Section 3, we must consider the available resources, which may be fragmented as we show in Figure 7.

To select a model, we must consider the interplay between the design decisions and runtime considerations. Our design decisions include: 1) Size and number of upstream models, 2) Size and architecture of the upstream model, 3) Relative importance of the upstream and downstream models, and 4) Output granularity. Although our ensemble architectures work on the block level, where upstream models are a prefix of the models, which highly discretize the problem, the problem is still not trivial. Picking the right size upstream model involves navigating a trade-off between model size, processing latency, and accuracy. For instance, as shown in Figure 3 and Table 3, using the first six blocks of the EfficientNetB0 barely adds any accuracy despite having $3.47\times$ more parameters. However, picking small models may actually lead to worse latency, as shown in Figure 5c, as earlier models have larger intermediate representations, an issue highlighted in earlier research [20]. Additionally, deciding the size and relative importance of the downstream models is also nontrivial, as they are highly dependent on the available resources and failure type. For instance, as we show in Table 5, picking a larger downstream model may not always increase the accuracy. Moreover, emphasizing training the accuracy of the downstream model by giving it higher relative importance may not yield higher accuracy, as we highlight in Table 6.

B.1 Ensemble Model Selection

Due to the complexity of “right-sizing” the model ensemble at training time, as the available resources and failure are hard to know beforehand. Our approach, similar to previous work [55, 1], trains a family of multiple model ensembles and selects the appropriate model at runtime. Algorithm 1 lists an exemplar heuristic that creates a family of trained ensembles. The algorithm takes the original architecture, possible architectures for the upstream model, and a resource budget. The resource budget can be a memory size or a latency SLO that the model must respect. To select the model family, we first iterate over the original model blocks and possible downstream architectures. We assume that the downstream architectures come in different sizes (e.g., number of filters in a CNN or number of hidden layers in a fully connected model). Next, we check if the selected number of blocks and the downstream architecture respect the resource budget. Lastly, the user can train these models and apply different granularities for models that have low accuracy. At runtime, systems can use a placement algorithm (e.g., a worst-fit heuristic). However, evaluating the performance of such runtime selection and placement approaches is part of our future work.

Algorithm 1: Ensemble_Family()

Input: Original model architecture O , Upstream models architectures A , Resource budget \mathcal{R} .

Output: Ensemble Family E .

```
1 Initialization:  $E \leftarrow []$ ;  
2 for  $\mathcal{B} \in O.Blocks$  do // Iterate over Blocks.  
3   for  $\mathcal{A} \in A$  do // Iterate over upstream architectures.  
4     if  $feasible(\mathcal{B}, \mathcal{A}, \mathcal{R})$  then // Ensembles must be within the resource budget.  
5        $E.append(\mathcal{B}, \mathcal{A})$ ;  
6 return  $E$ 
```

B.2 System Implementation

In this section, we detail the implementation of our failure-resilient model serving system. Although our multi-level model ensembles can be deployed on any AI inference systems, our current implementation is based on ONNX Runtime environment v1.21. After training the models using Pytorch v2.5.1, we export the sub-models into ONNX format and run them using the ONNX runtime. We export sub-models individually to different files and allow the users to send inference requests and for sub-models to exchange intermediate representation via a gRPC interface. The ONNX runtime allows for multiple execution providers. Our evaluation focuses on `CPUExecutionProvider` that allows running the models on CPUs and `CUDAExecutionProvider` that allows the models to run on GPUs using CUDA and cuDNN implementations. Our model inference implementation, which we plan to open-source, is $\sim 1k$ SLOC. Note that our current evaluation is limited to inference latency across different architectures and ensemble sizes, evaluating failure resiliency metrics, such as mean time to recovery (MTTR), and strategies such as warm and cold backups are part of our future work.

C Experimental Setup

In this section, we detail our datasets, architectures, training configuration, and compute resources for training and inference.

C.1 Datasets

Our training methodology is a general training methodology that applies to any data. In addition to the datasets listed in [Table 1](#), we add the BookCorpus dataset [\[63\]](#). Here we detail the four publicly available datasets we used.

- **CIFAR-100** [\[24\]](#): The CIFAR-100 dataset contains 60k 32×32 images and has 100 classes, grouped into 20 superclasses, *e.g.*, the **fruit and vegetables** class has **apples, mushrooms, oranges, pears, sweet peppers**. We use this dataset for an image classification task, and report performance in terms of Top-1 accuracy.
- **Tiered-ImageNet** [\[39\]](#): The Tiered-ImageNet dataset is a subset of ImageNet with 774k samples representing 608 classes, grouped into 34 higher-level nodes in the ImageNet human-curated hierarchy. However, we re-partitioned the training, validation, and test data to ensure that the model was exposed to all label classes, which was not a requirement in the original dataset construction. We use this dataset for an image classification task, and report performance in terms of Top-1 accuracy.
- **Speech Commands** [\[53\]](#): The Speech Commands dataset contains 65k (1-sec) recordings at 16kHz across 35 classes (*i.e.*, *words*). The dataset is used for classification and Speech Recognition, where we report Top-1 accuracy and Word Error Rate (WER), respectively.
- **BookCorpus** [\[63\]](#): Lastly, the BookCorpus dataset is composed of 11k novels comprising 1.2B tokens (using a vocab size of 8000), and we use this dataset for LLM Pre-Training, where we report the model perplexity.

C.2 Architectures

As highlighted in [Section 4.1](#), we use several architectures to validate our training approach. [Table 9](#) lists the models and the architecture used for our evaluation. The table also highlights the number of blocks in the

Table 9: Models architectures and number of blocks in the original model.

Model	Architecture	Blocks
EfficientNet-B0	CNN	7
ResNet50	CNN	4
ViT-B/16	Transformer	12
DeepSpeech2	GRU	6
GPT-mini	Transformer	8

Table 10: Training Configurations. BS is the batch size. LR is the learning rate reporting as starting learning rate with 10 warmup epochs and a cosine rate decay schedule. FT is a fine-tuning step for fine-tuning the downstream model. *For BookCorpus, batch size is reported in tokens per update, and training/fine-tuning steps reflect total token count.

Dataset	Architectures	BS	Learning Rate	Training Epochs	FT Epochs
CIFAR-100	EfficientNet-B0 (<i>Small</i>)	64	0.005	100	-
	EfficientNet-B0 ($\mathcal{B}1 - \mathcal{B}7$)	64	0.005	150-200	50
	EfficientNet-B0 (Three-upstream)	64	0.005	200	50
	Resnet50 (<i>Small</i>)	64	0.005	100	-
	Resnet50 ($\mathcal{B}1 - \mathcal{B}3$)	64	0.005	150-200	50
	Resnet50 (Three-upstream)	64	0.005	200	50
	ViT-B/16 (<i>Small</i>)	64	0.0001	150	-
	ViT-B/16 ($\mathcal{B}1 - \mathcal{B}6$)	64	0.0001	150-250	50
TieredImageNet	ViT-B/16 (Three upstream)	64	0.0001	250	50
	EfficientNet-B0	128	0.005	150-200	50
Speech-commands	EfficientNet-B0	64	0.001	100	30
	DeepSpeech2	64	0.001	100	30
BookCorpus	GPT-mini	65000*	0.0006	13.1 billion*	1.6 billion*

original model. Note that although there is no technical limit on the number of blocks, we limit the blocks based on the description of the original paper.

C.3 Training Configurations

In this section, we detail the training configurations, summarized in Table 10. For each dataset, the same configuration is shared between model sizes and configurations. As highlighted earlier, our ensemble models are trained in two steps. In the first step, we train the entire ensemble using a weighted loss function as explained in Section 2. Then we also fine-tune the downstream model while freezing upstream models, which further improves the results as we highlight later in Table 11. In all the training and fine-tuning steps, we use the AdamW[31] optimizer with the cosine schedules[30].

C.4 Training environment

We train models in a local SLURM cluster with many GPU types. The detailed cluster configuration is (***url hidden for anonymity***) Most of the training uses a single GPU except for classification on TieredImageNet and language modeling on BookCorpus, which is done using 2 and 4 GPU nodes respectively. The training is implemented using PyTorch v2.5.1 and is based on the TIMM[54] and other open-source implementations, which includes various architectures like ResNet, EfficientNet, and Vision Transformers. MEL models of EfficientNet and Resnet takes 5-10 hours to train on a single GPU on CIFAR-100 depending on the size (i.e. sub-blocks in the model). Training Vision Transformer and training on the TieredImageNet takes much longer around 15-24 hours on multiple GPUs. We plan to open-source our training scripts.

C.5 AI inference environment

Our AI inference environment is based on a local cluster of four machines with three Nvidia A2 GPUs running CUDA v12.4 and cuDNN v9.8.0. The machines are Dell PowerEdge servers with Intel(R) Xeon(R) CPU E5-2660 v3 @ 2.60GHz processor and connected via a 10 Gbps network. We evaluate the performance of

Table 11: Effect of hierarchical training. Reducing task complexity improves the accuracy of *small* models ($h_{\{1\}}, h_{\{2\}}$). However, note that models trained on different granularities are not directly comparable, as they solve slightly different problems.

Dataset	DNN Model	Fine-Grain Labels			Coarse-Grain Labels		
		$h_{\{1\}}$	$h_{\{2\}}$	$h_{\{1,2\}}$	$h_{\{1\}}$	$h_{\{2\}}$	$h_{\{1,2\}}$
CIFAR-100	EfficientNet-B0 ($\mathcal{B3}$)	0.5824	0.5885	0.7169	0.6966	0.7029	0.6033
	Resnet50 ($\mathcal{B2}$)	0.6523	0.6488	0.6820	0.7013	0.7121	0.6516
	ViT-B/16 ($\mathcal{B1}$)	0.4644	0.4667	0.5066	0.5782	0.5865	0.5111
	ViT-B/16 ($\mathcal{B2}$)	0.5583	0.5652	0.5937	0.6802	0.6820	0.5954
	ViT-B/16 ($\mathcal{B3}$)	0.5744	0.5860	0.6103	0.6975	0.7081	0.6109
	ViT-B/16 ($\mathcal{B4}$)	0.5892	0.5908	0.6167	0.7015	0.7197	0.6231
	ViT-B/16 ($\mathcal{B5}$)	0.5909	0.5960	0.6250	0.7147	0.7201	0.6279
	ViT-B/16 ($\mathcal{B6}$)	0.6030	0.6034	0.6295	0.7196	0.7284	0.6350
TieredImageNet	EfficientNet-B0 ($\mathcal{B4}$)	0.6007	0.6048	0.6430	0.7620	0.7704	0.6210
	EfficientNet-B0 ($\mathcal{B5}$)	0.6367	0.6359	0.6771	0.8123	0.8222	0.6904
	EfficientNet-B0 ($\mathcal{B6}$)	0.6957	0.7096	0.7420	0.8270	0.8342	0.7249

our architecture by evaluating the local performance on a GPU and a CPU, as well as evaluating the model serving system by deploying the models across servers.

D Additional Evaluation Results

D.1 Hierarchical training across sizes

Table 11 expands our results in Table 4. The table illustrates the effect of using coarse-grain labels as a design decision while training upstream models in the MEL framework. As shown, *reducing the task complexity helps create better performance across the upstream models, without compromising much performance on the downstream task, when the models are sufficiently big*. In some cases, hierarchical training even leads to better overall performance. For example, EfficientNet-B0 ($\mathcal{B5}$) on TieredImageNet yields a 1.4% improvement in accuracy on the fine-labels while achieving 82.2% performance on the upstream models. Similar results are also observed across multiple configurations of Vision Transformer models on CIFAR-100.

E Additional Ablation Studies

In this section, we extend our ablation studies by showing the performance of MEL when using 3 upstream model architectures and asymmetrical upstream model design.

E.1 Three ensembles

Figure 6 shows the scenario where we build an ensemble based on three upstream models. In this case, we require four downstream models for different model pairs, and in a situation where all three succeeded. Table 12 lists the accuracy of MEL when training three upstream models across different architectures on CIFAR-100. The results show that: *Adding more models always increased the overall accuracy with little to no effects on the individual upstream models or the downstream models*. For example, using three upstream models for EfficientNet-B0 ($\mathcal{B5}$) increases the accuracy by 1.44%, while typically being able to retain the accuracy of the upstream models, as in the case of two models.

E.2 Asymmetrical upstream models

Resource availability may be heterogeneous as highlighted in Figure 7, requiring the models to have different upstream sizes. To address this and as a primary step to the limitations introduced in Section 5, we discuss Table 13 that demonstrates MEL flexibility to build asymmetric ensemble models for diverse and resource-fragmented scenarios. The table shows the accuracy of multiple scenarios when training on the CIFAR-100 dataset. As shown, our training approach highlights that the trained models are not only able to refine each other, but this performance is also similar to a symmetrically designed ensemble model. As a specific example, EfficientNet-B0 ($\mathcal{B4}$ - $\mathcal{B5}$) achieves within 1% of the performance as compared to EfficientNet-B0 ($\mathcal{B5}$) from Table 3 while utilizing asymmetrically distributed, but similar number of parameters (memory budget).

Table 12: Performance of three upstream based MEL models. Top-1 Acc. is reported for classification task on CIFAR-100 on (1) individual upstream models (e.g. $h_{\{1\}}$) (2) “2-combination” downstream model (i.e. when two of the models are available e.g. $h_{\{1,2\}}$) and (3) the downstream model when all the upstreams are available $h_{\{1,2,3\}}$.

DNN Model	MEL									
	$h_{\{1\}}$	$h_{\{2\}}$	$h_{\{3\}}$	Para.	$h_{\{1,2\}}$	$h_{\{1,3\}}$	$h_{\{2,3\}}$	Para.	$h_{\{1,2,3\}}$	Para.
EfficientNet-B0 ($\mathcal{B}1$)	0.1965	0.1852	0.2149	4.08K	0.2249	0.2527	0.2449	11.45K	0.2675	27.03K
EfficientNet-B0 ($\mathcal{B}2$)	0.4036	0.4181	0.4458	21.59K	0.4615	0.4819	0.4816	48.08K	0.5010	86.77K
EfficientNet-B0 ($\mathcal{B}3$)	0.5692	0.5781	0.5835	0.07M	0.6205	0.6281	0.6274	0.15M	0.6481	0.24M
EfficientNet-B0 ($\mathcal{B}4$)	0.6780	0.6859	0.6887	0.32M	0.7242	0.7263	0.7284	0.65M	0.7443	1.02M
EfficientNet-B0 ($\mathcal{B}5$)	0.6938	0.7209	0.7477	0.88M	0.7552	0.7751	0.7811	1.79M	0.7913	2.69M
EfficientNet-B0 ($\mathcal{B}6$)	0.7273	0.7578	0.7502	2.90M	0.7870	0.7808	0.7953	5.83M	0.8042	8.86M
Resnet50 ($\mathcal{B}1$)	0.4962	0.5680	0.5691	0.25M	0.5760	0.5911	0.5955	0.55M	0.6182	0.98M
Resnet50 ($\mathcal{B}2$)	0.6442	0.6328	0.6805	1.40M	0.6712	0.7030	0.6987	3.30M	0.7152	4.95M
Resnet50 ($\mathcal{B}3$)	0.7470	0.6552	0.6977	8.76M	0.7654	0.7612	0.7280	17.50M	0.7761	26.86M
ViT-B/16 ($\mathcal{B}1$)	0.4497	0.4446	0.4564	7.80M	0.4965	0.4956	0.4975	15.90M	0.5199	24.42M
ViT-B/16 ($\mathcal{B}2$)	0.5495	0.5596	0.5450	14.90M	0.5882	0.5826	0.5855	30.00M	0.6053	45.68M
ViT-B/16 ($\mathcal{B}3$)	0.5586	0.5674	0.5706	22.00M	0.5959	0.5985	0.6039	44.30M	0.6163	66.93M
ViT-B/16 ($\mathcal{B}4$)	0.5802	0.5840	0.5784	29.17M	0.6132	0.6055	0.6089	58.49M	0.6227	88.19M

Table 13: Asymmetric MEL evaluation on CIFAR-100. Performance of MEL with uneven sized upstream models on the CIFAR-100 dataset. \dagger Top-1 accuracy is reported for the image classification task.

DNN Model	MEL					
	$h_{\{1\}}$		$h_{\{2\}}$		$h_{\{1,2\}}$	
	Perf. \dagger	Para.	Perf. \dagger	Para.	Perf. \dagger	Para.
EfficientNet-B0 ($\mathcal{B}3$ - $\mathcal{B}4$)	0.5687	0.07M	0.7064	0.32M	0.7116	0.40M
EfficientNet-B0 ($\mathcal{B}3$ - $\mathcal{B}5$)	0.5690	0.07M	0.7558	0.88M	0.7624	0.95M
EfficientNet-B0 ($\mathcal{B}4$ - $\mathcal{B}5$)	0.6723	0.32M	0.7540	0.88M	0.7704	1.20M
Resnet50 ($\mathcal{B}1$ - $\mathcal{B}3$)	0.5453	0.25M	0.7331	8.76M	0.7359	9.02M
Resnet50 ($\mathcal{B}2$ - $\mathcal{B}3$)	0.6404	1.40M	0.7301	8.76M	0.7382	10.30M

F More Baselines

In this section, we expand the results of Section 4.4 to the case when the architecture consists of 3-upstream models.

F.1 Single failover replicas

Table 14 expands the results from Table 7 when considering three upstream models, showing the efficacy of our training approach. It highlights that our *training approach not only creates resilient models, but also creates models that behave well and sometimes better than individually trained models.*

F.2 Training strategies

Table 15 shows the performance of MEL across different training strategies with the same architecture for comparison in the case of ensemble models trained with three upstream models. We compare three training approaches: 1) Our proposed MEL, 2) standalone model training on the final accuracy, and 3) individually training upstream and downstream models. As shown, *training the model using our MEL approach creates a better model than training models as standalone or training them individually and then combining them.*

G More systems evaluation

In this section, we further evaluate the performance of our proposed multi-level ensemble models on CPU and the GPU, where ensemble models are hosted on the same server. Figure 8, Figure 9, and Figure 10 shows the performance of the models when we deploy them across multiple servers. As shown, when deploying the models on one server, increasing the number of layers always increases the processing latency. For instance, going from one block to five blocks in EfficientNet-B0, see Figure 5, increases the latency by 4.8ms and 8.9ms for the small and the MEL models, respectively. Moreover, the figures highlight that our proposed architecture

Table 14: Performance of individual backup models $h_{\{1\}}, h_{\{2\}}, h_{\{3\}}$ under joint optimization within the MEL framework for three upstream models compared to individual training.

DNN Model	MEL Perf.			Standalone
	$h_{\{1\}}$	$h_{\{2\}}$	$h_{\{3\}}$	
EfficientNet-B0 ($\mathcal{B}1$)	0.1965	0.1852	0.2149	0.2060
EfficientNet-B0 ($\mathcal{B}2$)	0.4036	0.4181	0.4458	0.4268
EfficientNet-B0 ($\mathcal{B}3$)	0.5692	0.5781	0.5835	0.5809
EfficientNet-B0 ($\mathcal{B}4$)	0.6780	0.6859	0.6887	0.7105
EfficientNet-B0 ($\mathcal{B}5$)	0.6938	0.7209	0.7477	0.7471
EfficientNet-B0 ($\mathcal{B}6$)	0.7273	0.7578	0.7502	0.7686
Resnet50 ($\mathcal{B}2$)	0.6442	0.6328	0.6805	0.6672
Resnet50 ($\mathcal{B}3$)	0.7470	0.6552	0.6977	0.7300
ViT-B/16 ($\mathcal{B}1$)	0.4497	0.4446	0.4564	0.4803
ViT-B/16 ($\mathcal{B}2$)	0.5495	0.5596	0.5450	0.5732
ViT-B/16 ($\mathcal{B}3$)	0.5586	0.5674	0.5706	0.5931
ViT-B/16 ($\mathcal{B}4$)	0.5802	0.5840	0.5784	0.6044

Table 15: Three upstream MEL. Performance of $h_{\{1,2,3\}}$ under different training strategies –Standalone trains only $h_{\{1,2,3\}}$, while Individually trained trains $h_{\{1\}}, h_{\{2\}}, h_{\{3\}}$ independently and then optimizes $h_{\{1,2,3\}}$ with frozen upstream models.

DNN Model	MEL Perf.	Standalone	Ind. Trained
EfficientNet-B0 ($\mathcal{B}1$)	0.2675	0.2880	0.2244
EfficientNet-B0 ($\mathcal{B}2$)	0.5010	0.5038	0.4636
EfficientNet-B0 ($\mathcal{B}3$)	0.6481	0.6345	0.6202
EfficientNet-B0 ($\mathcal{B}4$)	0.7443	0.7120	0.7393
EfficientNet-B0 ($\mathcal{B}5$)	0.7913	0.7367	0.7809
EfficientNet-B0 ($\mathcal{B}6$)	0.8042	0.7545	0.8001
Resnet50 ($\mathcal{B}2$)	0.7152	0.6225	0.6805
Resnet50 ($\mathcal{B}3$)	0.7761	0.6651	0.7515
ViT-B/16 ($\mathcal{B}1$)	0.5199	0.5160	0.5121
ViT-B/16 ($\mathcal{B}2$)	0.6053	0.5868	0.6038
ViT-B/16 ($\mathcal{B}3$)	0.6163	0.6039	0.6196
ViT-B/16 ($\mathcal{B}4$)	0.6227	0.6041	0.6309

typically uses more time than a small standalone model, as the ensemble models are much wider, hence requiring more processing time.

Most importantly, the figures highlight the performance of the ensemble model when deployed on three servers (*i.e.*, the intended deployment model). The results highlight a key aspect of deploying ensemble models. First, although using a smaller number of blocks leads to lower processing time and parameters. Our results, which are consistent with the results on split processing[20], show that only using a small block prefix may lead to higher response time. Nonetheless, the results show that once we go past the first couple of layers, the results stabilize our models only include a small overhead.

H Limitations

The main limitation of our work is that the number of models for the downstream tasks grows as $O(2^{\text{upstream models}})$ of the number of upstream models. For example, the ensemble with three upstream models (see Figure 6) requires 4 number of downstream models to handle different scenarios. One approach could be to train models using just one (or a limited number of) downstream models capable of executing without requiring all the representations from the upstream models. This could be achieved using a masking technique (*e.g.*, adding zeros for failed models) while training, however, such an approach requires a different training methodology and is left for future work.

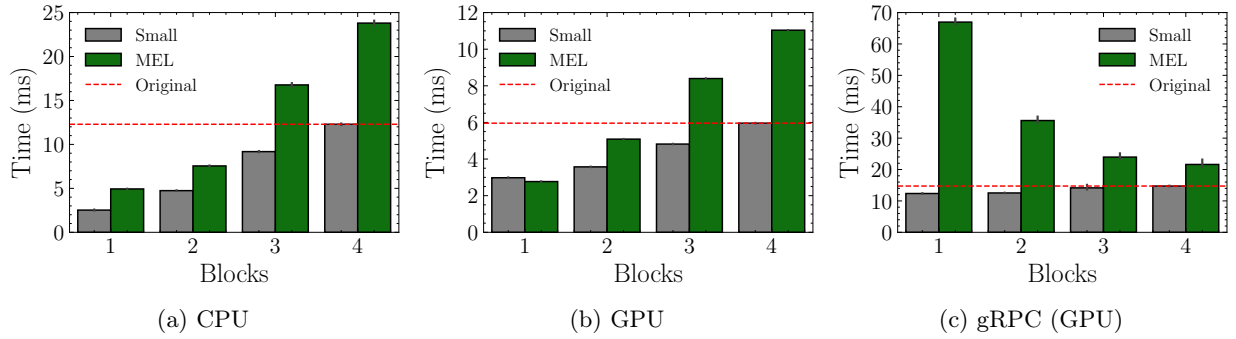


Figure 8: Processing Latency of ResNet50 on CIFAR-100.

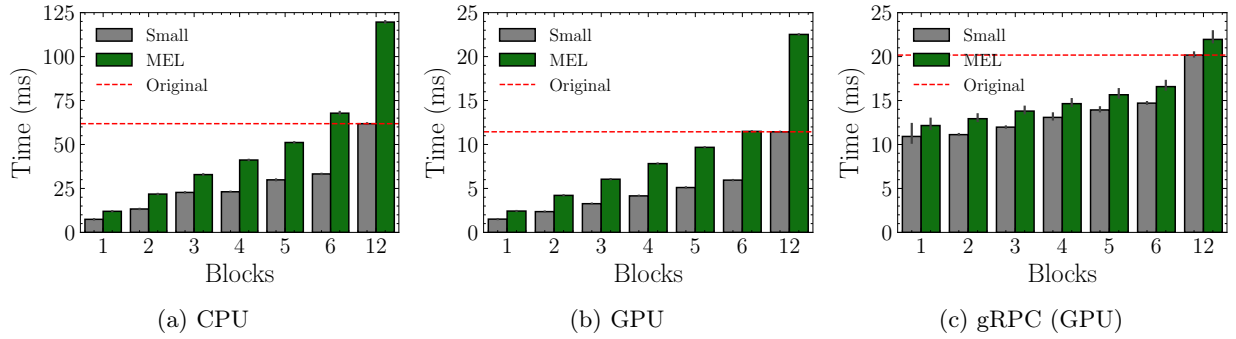


Figure 9: Processing Latency of ViT-B/16 on CIFAR-100.

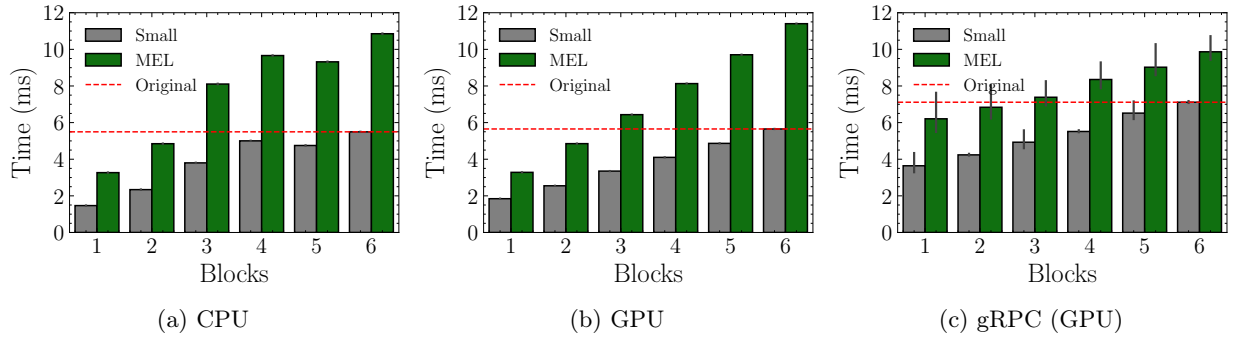


Figure 10: Processing Latency of DeepSpeech2 on Speech Commands.